




High Glucose and Carbonyl Stress Impair HIF-1-Regulated Responses and the Control of *Mycobacterium tuberculosis* in Macrophages

Graciela Terán,^{a*} Hanxiong Li,^a Sergiu-Bogdan Catrina,^{b,c} Ruining Liu,^a Susanna Brighenti,^d Xiaowei Zheng,^b Jakob Grünler,^b Susanne Nylén,^a Berit Carow,^{a*§}  Martin E. Rottenberg^a

^aDepartment of Microbiology, Tumor and Cell Biology (MTC), Karolinska Institutet, Stockholm Sweden

^bDepartment of Molecular Medicine and Surgery, Karolinska Institutet, Rolf Luft Research Center for Diabetes and Endocrinology, Karolinska University Hospital, Stockholm, Sweden

^cCenter for Diabetes, Academic Specialist Center, Stockholm, Sweden

^dCenter for Infectious Medicine (CIM), Department of Medicine, Karolinska Institutet, Stockholm, Sweden

Graciela Terán and Hanxiong Li contributed equally to this article. The author order was determined on the basis of seniority.

ABSTRACT Diabetes mellitus (DM) increases the risk of developing tuberculosis (TB), but the mechanisms behind diabetes-TB comorbidity are still undefined. Here, we studied the role of hypoxia-inducible factor-1 (HIF-1), a main regulator of metabolic and inflammatory responses, in the outcome of *Mycobacterium tuberculosis* infection of bone marrow-derived macrophages (BMM). We observed that *M. tuberculosis* infection of BMM increased the expression of HIF-1 α and HIF-1-regulated genes. Treatment with the hypoxia mimetic deferoxamine (DFO) further increased levels of HIF-1-regulated immune and metabolic molecules and diminished the intracellular bacterial load in BMM and in the lungs of infected mice. The expression of HIF-1-regulated immunometabolic genes was reduced, and the intracellular *M. tuberculosis* levels were increased in BMM incubated with high-glucose levels or with methylglyoxal (MGO), a reactive carbonyl compound elevated in DM. In line with the *in vitro* findings, high *M. tuberculosis* levels and low HIF-1-regulated transcript levels were found in the lungs from hyperglycemic *Lep^{rd/db}* compared with wild-type mice. The increased intracellular *M. tuberculosis* growth and the reduced expression of HIF-1-regulated metabolic and inflammatory genes in BMM incubated with MGO or high glucose were reverted by additional treatment with DFO. *Hif1a*-deficient BMM showed ablated responses of immunometabolic transcripts after mycobacterial infection at normal or high-glucose levels. We propose that HIF-1 may be targeted for the control of *M. tuberculosis* during DM.

IMPORTANCE People living with diabetes who are also infected with *M. tuberculosis* are more likely to develop tuberculosis disease (TB). Why diabetic patients have an increased risk for developing TB is not well understood. Macrophages, the cell niche for *M. tuberculosis*, can express microbicidal mechanisms or be permissive to mycobacterial persistence and growth. Here, we showed that high glucose and carbonyl stress, which mediate diabetes pathogenesis, impair the control of intracellular *M. tuberculosis* in macrophages. Infection with *M. tuberculosis* stimulated the expression of genes regulated by the transcription factor HIF-1, a major controller of the responses to hypoxia, resulting in macrophage activation. High glucose and carbonyl compounds inhibited HIF-1 responses by macrophages. Mycobacterial control in the presence of glucose or carbonyl stress was restored by DFO, a compound that stabilizes HIF-1. We propose that HIF-1 can be targeted to reduce the risk of developing TB in people with diabetes.

KEYWORDS diabetes, HIF-1, macrophage, *Mycobacterium tuberculosis*

Editor Barry R. Bloom, Harvard School of Public Health

Copyright © 2022 Terán et al. This is an open-access article distributed under the terms of the [Creative Commons Attribution 4.0 International license](https://creativecommons.org/licenses/by/4.0/).

Address correspondence to Martin E. Rottenberg, martin.rottenberg@ki.se.

*Present address: Graciela Terán, Universidad Mayor de San Andrés, La Paz, Bolivia.

§Present address: Berit Carow, Novavax AB, Uppsala, Sweden.

The authors declare no conflict of interest.

Received 19 April 2022

Accepted 31 August 2022

Published 19 September 2022

A quarter of the global population has been infected with *Mycobacterium tuberculosis*. However, only a fraction of infected individuals develops tuberculosis (TB). Still, in 2020, 10 million people developed the disease and 1.5 million died from TB (1). Why some individuals develop TB is not completely understood. However, human beings with a compromised immune system, such as people living with HIV, have a higher risk of developing TB.

Infection occurs when inhaled *M. tuberculosis* reaches the lung alveoli and is phagocytized by resident alveolar macrophages (2). Infected macrophages or those activated by bacterial molecules will recruit mononuclear phagocytes. A mantle of lymphocytes will then surround these phagocytes, forming a granuloma, in which bacterial growth is either restricted or disseminated to other organs and can be transmitted to uninfected individuals.

Type 2 diabetes (DM) is a metabolic disease characterized by high blood-glucose levels secondary to an inappropriate insulin secretion for peripheral insulin sensitivity. Inflammation secondary to infection or obesity worsens metabolic control secondary to an increase in insulin resistance. Different cell types cannot decline their glucose uptake when exposed to hyperglycemia leading to high intracellular glucose levels (3), resulting in increased synthesis of reactive carbonyl compounds, such as methylglyoxal (MGO), a by-product of glycolysis. MGO mediates rapid nonenzymatic glycation of proteins, lipids, and DNA to promote the formation of advanced glycation end products (AGEs), which eventually renders irreversible damage to these macromolecules, including their integrity of structure and function (4). MGO and MGO-derived AGE thus impact tissue and organ functions and are important factors in vascular complication development in DM (5).

Epidemiologic studies have revealed a 3-fold higher risk of active TB among patients with DM than among individuals without DM and a strong association between TB and DM regardless of TB endemicity (6–8). About 15% of TB cases globally are linked to DM (9). While people with DM are at higher risk of progressing from latent to active TB, TB might also contribute to the worsening of metabolic control in subjects with DM (10). An exacerbated immunopathology is a frequent observation in TB that is complicated by DM (11). However, the underlying mechanisms behind the DM-TB association are largely unknown.

The adaptive response of mammalian cells to the stress of oxygen depletion is coordinated by the action of hypoxia-inducible transcription factors (HIFs). The alpha subunits of these transcription factors serve as the central sensor of oxygen tension in cells. HIFs function is regulated at least in part at the protein level via the degradation of the HIF- α subunits under normoxic conditions. The hydroxylation of proline residues of HIF- α is executed by prolyl-hydroxylases (PHDs) that use Fe²⁺, oxygen, and oxoglutarate as cofactors (12–14). The hydroxylated form of HIF- α binds to the von Hippel-Lindau (VHL) tumor suppressor protein that is part of an E3 ubiquitin ligase complex that targets HIF- α for proteasomal degradation (12, 15). Under hypoxia HIF- α , prolyl hydroxylation is inhibited, and HIF accumulates in the nucleus and transactivates HIF-responsive genes (16).

A number of isoforms of the α -subunit have been identified, but the main important functionality is HIF-1 α and HIF-2 α with both distinct and overlapping biological roles. HIF-1 has been shown to induce apoptotic pathways and drive the expression of genes that are involved in the glycolytic pathway, whereas HIF-2 preferentially promotes growth and angiogenesis (17, 18). HIFs are highly relevant to the proper function of different immune cell populations, including macrophages (19). Macrophages activated by microbial infection or by several innate receptor agonists switch their metabolism from oxidative phosphorylation to glycolysis, a response that is similar to the response to hypoxia. HIF-1 contributes to the expression of genes associated with macrophage activation (19, 20). Some of these HIF-1-regulated immune molecules, such as inducible nitric oxide synthase (iNOS) or interleukin-1 β (IL-1 β), have central roles in the intracellular control of *M. tuberculosis* (21, 22). HIF-1 has been shown to accumulate in the human hypoxic TB granuloma (23), and TB lesions in experimental animals show

an increase in glycolytic pathways with a reduction of the tricarboxylic acid cycle and oxidative phosphorylation (24). Mice deficient in HIF-1 in myeloid cells showed higher susceptibility to infection with *M. tuberculosis* (25).

In the lung of infected individuals, *M. tuberculosis*-specific T cells will recognize infected macrophages and secrete interferon- γ (IFN- γ), required for macrophage activation, further inducing iNOS expression and containment of infection (26–28). Moreover, HIF-1 was shown to regulate IFN- γ responses of *M. tuberculosis*-infected macrophages; however, *hif1a*-deficient macrophages permitted the growth of *M. tuberculosis* even when activated with IFN- γ (25, 29).

Hyperglycemia has been shown to repress HIF-1 function (30), and a defective reaction of tissues to hypoxia due to HIF-1 inhibition has been suggested to be a pathogenic mechanism in DM (31, 32).

Here, we hypothesize that an impaired HIF-1 function during DM would aggravate *M. tuberculosis* infection in mice by hampering protective immune responses. We showed that bone marrow-derived macrophages (BMM) express high levels of HIF-1-regulated genes after infection with *M. tuberculosis* or *M. bovis* BCG. Treatment with the hypoxia mimic deferoxamine (DFO) increased immunometabolic responses in infected BMMs and in the lungs of *M. tuberculosis*-infected mice. DFO treatment reduced the *M. tuberculosis* titers in BMM treated or not with IFN- γ and decreased the bacterial load in the lungs of infected mice. The incubation with either MGO or high-glucose concentrations hampered the expression of HIF-1-regulated genes and impaired bacterial control in *M. tuberculosis*-infected BMM. Treatment with DFO restored HIF-1-regulated responses to infection and improved *M. tuberculosis* control in MGO and high-glucose-treated cells.

RESULTS

HIF-1-dependent responses increase in mycobacteria-infected BMM and in lungs of *M. tuberculosis*-infected mice. We first analyzed the expression of HIF-dependent responses during infection of BMM with mycobacteria. The expression of *hif1a* mRNA and HIF-1 α protein was enhanced in the attenuated *M. bovis* BCG-infected BMM (Fig. 1A to C and Fig. S1A in the supplemental material). The expression levels of HIF-1-regulated *vegfa* and the glycolytic transcripts *pdk1* and *ldha* mRNA were also increased in *M. tuberculosis*-infected BMM (Fig. 1D to F). In line with this, lactate, the final product of glycolysis was increased in BCG-infected BMM (Fig. 1G). HIF-1 has been shown to induce *il1b* and *inos* expression and increase nitric oxide (NO) production (20, 33), and *il1b* and *inos* mRNA and the nitrite concentration were increased in BMM at different times after infection with BCG (Fig. 1H to J). The infection of BMM with virulent *M. tuberculosis* also increased the levels of HIF-1 α mRNA and protein expression (Fig. 1K to M). HIF-1 regulated glycolytic transcripts (Fig. 1N and O) and *il1b* and *inos* transcripts (Fig. 1P and Q), and the levels of nitrite (Fig. 1R) were all increased in *M. tuberculosis*-infected BMM.

The expression of HIF-1-regulated metabolic genes was then evaluated in the lungs of C57BL/6 mice infected with *M. tuberculosis* via the aerosol route. We found that levels of *hif1a*, *glut1*, and *vegfa* mRNA were all elevated after infection with *M. tuberculosis* (Fig. S1B and D).

DFO enhances HIF-1-regulated responses and *M. tuberculosis* control in BMM. DFO is an iron chelator that stabilizes HIFs by inhibiting PHDs (34). Treatment of BMM with 100 μ M DFO for 24 h increased the expression of HIF-1 α (Fig. 2A and B). Using a HIF-1 reporter assay, we observed that DFO increased HIF-1 activity in macrophages before or after infection with BCG (Fig. 2C). BCG-infected BMM were treated with 100 μ M DFO 4 h after infection. The concentration of *glut1*, *vegfa*, *pdk1*, and *ldha* mRNAs in uninfected BMM was increased after DFO treatment (Fig. 2D to G) and DFO further increased levels of these transcripts in BCG-infected BMM (Fig. 2D to G). *il1b* and *inos* mRNAs (Fig. 2H and I) and nitrite levels in the culture supernatants (Fig. 2J) were also increased after DFO treatment of infected BMM. DFO stimulation of uninfected cells resulted in low *il1b*, *inos* mRNA, and nitrite in supernatants compared to that of mycobacteria-infected BMM (Fig. 2H to J). The levels of lactate were also

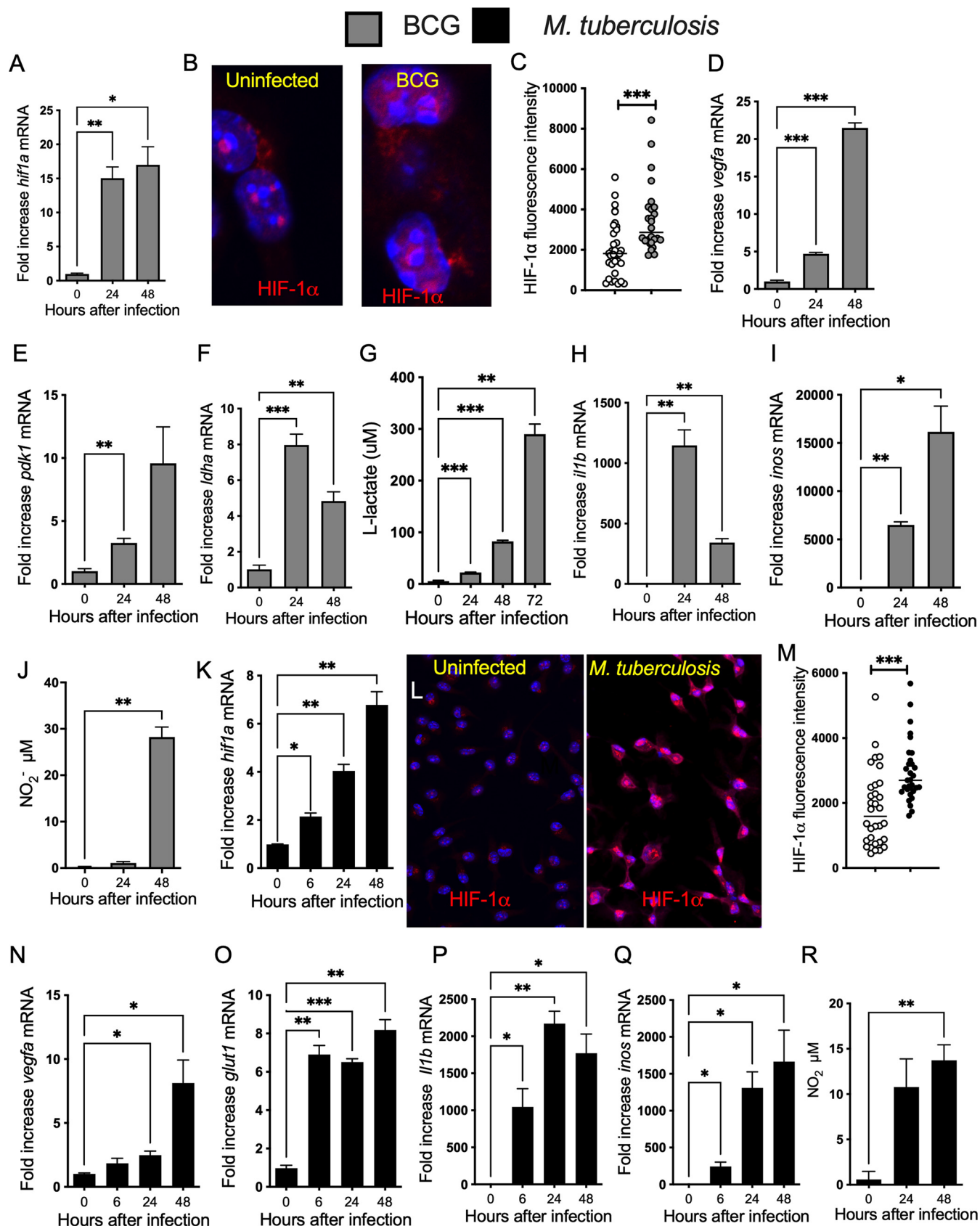


FIG 1 HIF-1-regulated responses increase in mycobacteria-infected BMM. (A, D to F, H, I, K, and N to Q) Total RNA was extracted from triplicate independent cultures of BMM before and at different time points after infection with BCG (A, D to F, H, and I) or *M. tuberculosis* (K and N to Q) at an MOI (Continued on next page)

elevated in supernatants of mycobacteria-infected BMM treated with DFO, whereas coincubation with 2-DG, an inhibitor of glycolysis, reduced the lactate levels in culture supernatants (Fig. 2K). DFO treatment of *M. tuberculosis*-infected BMM also increased the levels of HIF-1 α (Fig. 2L) and metabolic and inflammatory transcripts (Fig. 2M to O), as well as nitrite levels in the culture supernatants (Fig. 2P).

We next studied, whether DFO also increased the levels of HIF-1-regulated transcripts *in vivo*. For this purpose, mice were administered intraperitoneally (i.p.) with 400 mg/kg DFO every other day and sacrificed the day after the last dose. The levels of *glut1* and *vegfa* mRNA in lungs, spleens, and livers were elevated in DFO-treated mice (Fig. S2A, B, D, E, and H). In addition, the levels of *inos* mRNA in livers, but not lungs and spleens, of DFO-treated mice were found to be increased (Fig. S2C, F, and I).

Then, we investigated whether DFO administration every other day for 3 months altered the outcome of *M. tuberculosis*-aerosol infection in mice. We found that DFO-treated mice showed reduced levels of *M. tuberculosis* in lungs (Fig. 3A). In line with these results, levels of *hif-1a*, *vegfa*, *glut1*, and *inos* mRNA were elevated in the lungs of *M. tuberculosis*-infected, DFO-treated mice (Fig. 3B to E) compared to DFO-untreated, -infected controls. Levels of *il1b* showed a trend toward increased levels without reaching statistical significance (Fig. 3F).

The effect of DFO in the control of intracellular *M. tuberculosis* growth was then tested. The intracellular levels of green fluorescent protein (gfp)-expressing *M. tuberculosis* and the frequency of infected cells increased with the multiplicity of infection (MOI) used and with the time after infection, as also observed when evaluating *M. tuberculosis* infection on adherent BMM (Fig. S3A to F). Preincubation of cells with IFN- γ did not alter the bacterial uptake when measured 4 h after infection (Fig. S3G) but reduced the levels of intracellular *M. tuberculosis* and the percentage of infected BMM when measured 5 days after infection (Fig. S3H). The incubation of BMM with DFO reduced the intracellular load and percentage of infected cells 5 days after infection compared to controls (Fig. 3G to I). Moreover, the culture of BMM with both DFO and IFN- γ further reduced the intracellular *M. tuberculosis* load compared to BMM treated with either IFN- γ or DFO alone (Fig. 3G to I). DFO did not hamper the growth of *M. tuberculosis* in axenic cultures at the concentrations used in the BMM cultures (Fig. S3I).

MGO hampers HIF-1 responses and the growth control *M. tuberculosis* in BMM.

Methylglyoxal (MGO), a highly reactive α -oxoaldehyde and dicarbonyl formed as a by-product of glycolysis, is increased in the setting of high glucose in DM (35). Whether MGO hampers the HIF-regulated responses of *M. tuberculosis*- or BCG-infected BMM and the intracellular growth of *M. tuberculosis* was then analyzed. MGO was toxic for *M. tuberculosis*-infected or -uninfected BMM at 1,000 μ M but not at 750 μ M or lower concentrations as determined by LDH release assay or live/dead staining (Fig. S4A and B). We found that incubation of BCG-infected BMM with MGO reduced HIF-regulated *vegfa*, *il1b*, and *inos* transcripts (Fig. 4A to C), as well as the levels of nitrite in culture supernatants (Fig. 4D). Treatment with MGO also reduced inflammatory and metabolic transcripts levels in *M. tuberculosis*-infected BMM (Fig. 4E to G). Similar to observations in BCG-infected cells, the levels of lactate were increased in *M. tuberculosis*-infected BMM compared to controls and were decreased in MGO-treated BMM (Fig. 4H). The incubation of BMM with MGO did not modify the uptake of *M. tuberculosis* (Fig. S4C)

FIG 1 Legend (Continued)

of 5:1. The relative concentration of *hif1a* (A and K), *vegfa* (D and N), *pdk1* (E), *ldha* (F), *glut1* (O), *il1b* (H and P), and *inos* (I and Q) transcripts in relation to *hprt* mRNA levels in the same sample was determined by real-time PCR. Differences with noninfected controls are significant at *, $P \leq 0.05$; **, $P \leq 0.01$; and ***, $P \leq 0.001$, Student's *t* test. (B, C, L, and M) Micrographs showing labeling for HIF-1 α in BMM 24 h after either BCG (B) or *M. tuberculosis* (I) infection and in uninfected controls (DAPI was used for nuclear staining). The HIF-1 α label intensity in BMM 24 h after infection with BCG (C) or *M. tuberculosis* (M) infected BMM was quantified using the Cell Profiler software. The quantification was performed in 3 independent samples (4 field of view per sample). The individual and the mean HIF-1 α levels per cell in one field of view are shown. Differences are significant at ***, $P \leq 0.001$, unpaired Student's *t* test. (G) The lactate concentration accumulated in the supernatants from BMM infected with *M. bovis* BCG (MOI 1:1) was measured by lactate dehydrogenase assay. The data represent the results of triplicate independent cultures \pm SEM. A representative of 2 experiments is shown. Differences with noninfected controls are significant at **, $P \leq 0.01$ and ***, $P \leq 0.001$, unpaired Student's *t* test. (I and R) The concentration of nitrite in the supernatants of either *M. tuberculosis* (I) or BCG-infected (R) BMM was measured at different times after infection. The mean levels of NO₂⁻ \pm SEM in independent triplicates were measured by Griess assay.

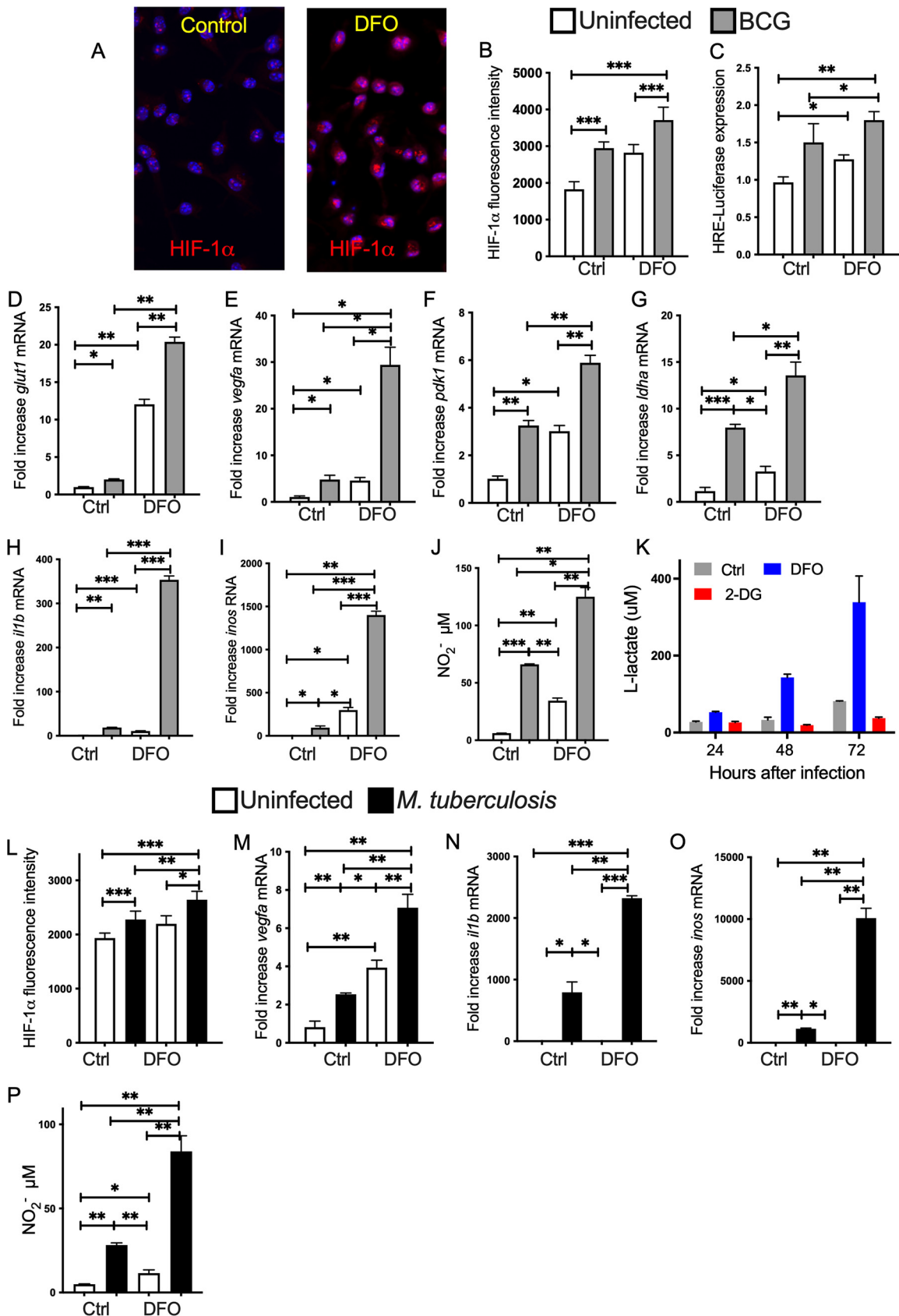


FIG 2 DFO stimulates HIF-1-mediated immune and metabolic responses in BCG and *M. tuberculosis*-infected BMM. (A and B) BMM were infected with BCG and treated with 100 μ M DFO starting 4 h after infection or left untreated. (A) The micrograph of HIF-1 α (Continued on next page)

but resulted in higher intracellular bacterial levels and frequencies of infected BMM at 5 days after infection (Fig. 4I to K). The bacterial levels of IFN- γ -treated BMM increased when coincubated with MGO albeit displaying lower *M. tuberculosis* levels than BMM incubated with MGO alone (Fig. 4I to K). The uptake of *M. tuberculosis* in IFN- γ -treated BMM treated or not with MGO was similar (Fig. S4C).

Despite the reduced HIF-regulated transcripts and the increased intracellular growth of *M. tuberculosis* in MGO-treated BMM, MGO treatment of BMM increased the HIF-1 α protein levels when measured before and after infection with *M. tuberculosis* (Fig. 4L and M), suggesting that the reduced levels of HIF-1-regulated transcripts are not due the destabilization of HIF-1 α . However, the transcriptional activity of HIF-1, as measured by a luciferase reporter, was reduced by incubation with 400 μ M MGO before or after BCG infection of macrophages (Fig. 4N).

Impaired HIF-1-responses and *M. tuberculosis* control in high-glucose-treated BMM and in hyperglycemic *Lepr^{db/db}* mice in vivo. We then studied whether incubation of mycobacteria-infected BMM in a high-glucose concentration altered the accumulation of HIF-1-dependent transcripts. For this purpose, BMM were cultured in either 5 mM or 25 mM glucose for 3 days before infection with BCG. We observed that levels of *glut1*, *vegfa*, *il1b*, and *inos* transcripts were all reduced in mycobacteria-infected BMM when cultured in 25 mM compared to those cultured in 5 mM glucose (Fig. 5A to D).

Leptin receptor-deficient *Lepr^{db/db}* mice develop significant obesity, fasting hyperglycemia, and hyperinsulinemia and are a model for type 2 DM (36). *Lepr^{db/db}* mice showed enhanced *M. tuberculosis* loads in lungs when measured 12 weeks postinfection (Fig. 5E). As expected, *Lepr^{db/db}* were weightier and showed higher levels of blood glucose and HbA1c than C57BL/6 controls before and after *M. tuberculosis* infection that were compatible with those that characterize DM (Fig. 5F to H). HbA1c levels were higher in *Lepr^{db/db}* mice after infection with *M. tuberculosis* (Fig. 5H).

Immune and metabolic HIF-1-regulated transcripts were reduced in lungs from *M. tuberculosis*-infected *Lepr^{db/db}* compared to wild-type (WT) mice (Fig. 5I to L). Moreover, *ifng* and *il17a* transcripts were reduced while *tnf* mRNA levels (that are not regulated by HIF-1) were similar in mutant and WT-*M. tuberculosis*-infected mice (Fig. 5M to O).

DFO reverts the MGO-hampered HIF-1-mediated responses and the enhanced susceptibility to *M. tuberculosis* infection of BMM. We then tested whether DFO was able to revert the MGO-impaired metabolic and inflammatory responses and *M. tuberculosis* control. The frequency of infected cells as well as the intracellular bacterial loads was reduced by coincubation of DFO in MGO-treated BMM to levels similar to those registered in DFO-treated BMM (Fig. 6A to D). *vegfa*, *il1b*, and *inos* transcripts, as well as nitrite concentration in *M. tuberculosis*-infected BMM, were reduced when treated with MGO, but the addition of DFO restored these responses to levels similar to those determined in DFO-treated *M. tuberculosis*-infected BMM (which were, in turn, higher than untreated controls)

FIG 2 Legend (Continued)

immunolabeling 24 h after DFO treatment in noninfected cultures. The fluorescence intensity of HIF-1 α was determined in triplicate independent cultures (4 determinations per slide). (B) The mean HIF-1 α intensity per cell \pm SEM in one representative sample is shown. Differences are significant at *, $P \leq 0.05$; **, $P \leq 0.01$; and ***, $P \leq 0.001$, one-way ANOVA with Welch's correction. (C) The relative HRE activity in RAW macrophages treated or not with DFO was evaluated 24 h after BCG infection. The mean relative luciferase levels \pm SEM are in triplicated cultures are depicted. One of two experiments is depicted. Differences are significant at *, $P \leq 0.05$; **, $P \leq 0.01$; and ***, $P \leq 0.001$, one-way ANOVA with Welch's correction. (D to I) Total RNA was extracted 24 h after treatment and the levels of *glut1* (D), *vegfa* (E), *pdk1* (F), *ldha* (G), *il1b* (H), and *inos* (I) mRNA were measured by real-time PCR. The mean fold increase of mRNA concentration in triplicate cultures \pm SEM compared to an uninfected and untreated control \pm SEM is depicted. One out of at least 3 experiments is depicted. Differences are significant at **, $P \leq 0.01$ and ***, $P \leq 0.001$, one-way ANOVA test with Welch's correction. (J) The concentration of nitrite in the supernatants of BCG-infected and or DFO-treated BMM was measured 48 h after culture. The mean levels of NO $_2^-$ \pm SEM in independent triplicates was measured by Griess assay. Differences are significant at **, $P \leq 0.01$ and ***, $P \leq 0.001$, one-way ANOVA test with Welch's correction. (K) The lactate concentration was measured in the supernatants of BMM cultures after treatment with either 100 μ M DFO or 300 μ M 2-DG at different times after BCG infection. (L) HIF-1 α was labeled in BMM infected with *M. tuberculosis* and treated with 100 μ M DFO starting 4 h after infection or left untreated. The mean HIF-1 α intensity per cell \pm SEM in one representative of 3 independent samples is shown. Differences are significant at *, $P \leq 0.05$; **, $P \leq 0.01$; and ***, $P \leq 0.001$ one-way Welch's ANOVA. (M to O) The fold increase of *vegfa* (M), *il1b* (N), and *inos* (O) transcripts in BMM cultures 24 h after *M. tuberculosis* infection treated or not with DFO as indicated above ($n = 3$ per group) \pm SEM are depicted. Differences are significant at *, $P \leq 0.05$; **, $P \leq 0.01$; and ***, $P \leq 0.001$, one-way Welch's ANOVA test. (P) The concentration of nitrite in the supernatants of *M. tuberculosis*-infected and or DFO-treated BMM was measured 72 h after culture. Differences are significant at *, $P \leq 0.05$ and **, $P \leq 0.01$ one-way Welch's ANOVA test.

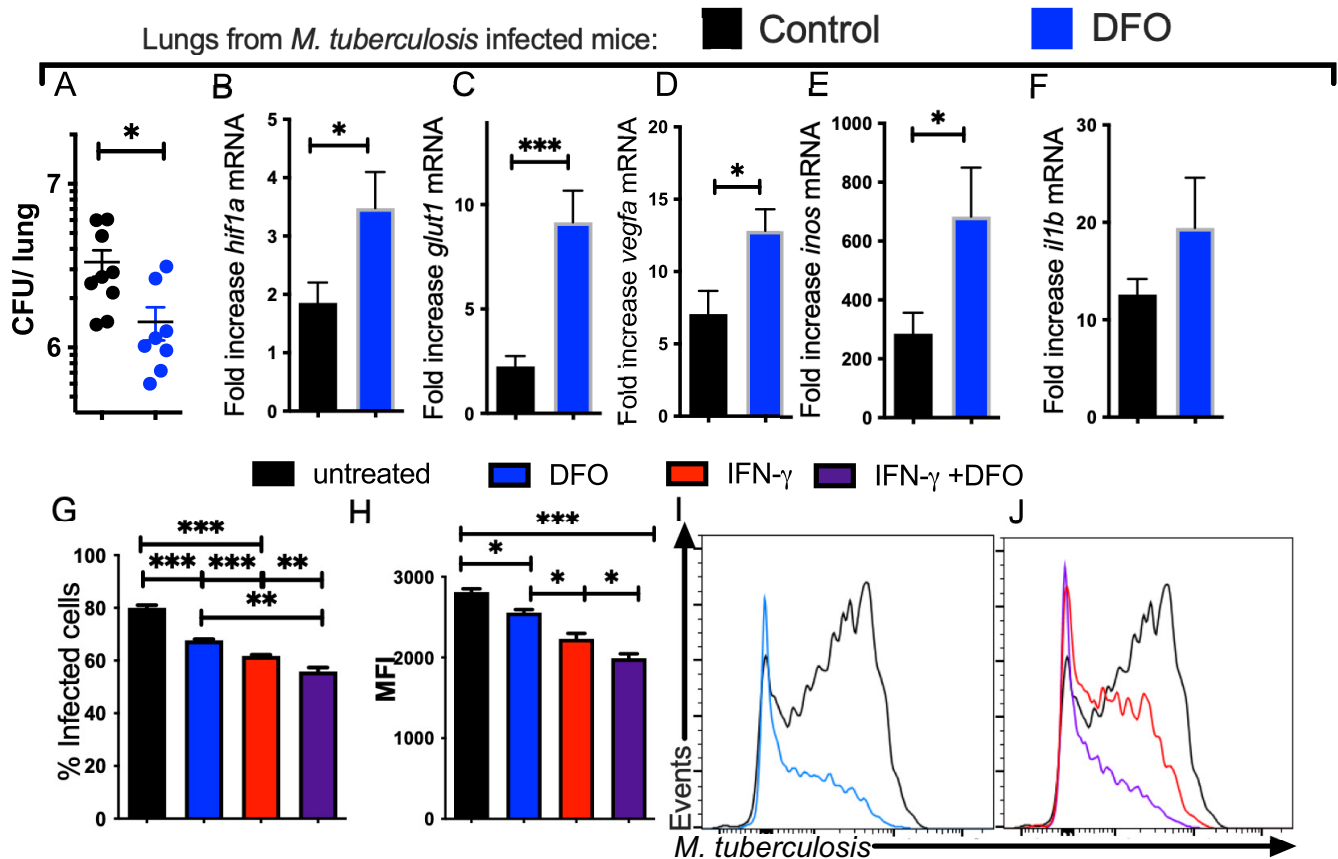


FIG 3 DFO treatment of BMM improves the intracellular growth control of *M. tuberculosis*. (A) C57BL/6 mice were treated with 400 mg/kg DFO i.p. every other day after aerosol infection with *M. tuberculosis* for 12 weeks. The group median and the individual CFU per lung of DFO-treated and untreated mice ($n = 9$ per group) are depicted (median CFU/lung: control $2.80 \cdot 10^6$; DFO treated: $7 \cdot 10^6$). Differences in CFU between DFO-treated and untreated groups are significant (*, $P < 0.05$, Mann-Whitney U test). (B to F) The mean relative levels \pm SEM of *hif1a* (B), *glut1* (C), *vegfa* (D), *inos* (E), and *il1b* (F) transcripts in lungs of DFO-treated or control mice ($n = 5$ per group) were measured by real-time PCR. The results were normalized with the level of a transcript in the lung of an untreated and uninfected control animal. Differences with the untreated group are significant at *, $P \leq 0.05$ and ***, $P \leq 0.001$, Student's t test with Welch's correction. (G to J) A group of BMM was treated with IFN- γ starting 48 h before *M. tuberculosis*-gfp infection (MOI 1:1). Groups of IFN- γ -activated and control BMM were incubated with DFO 4 h after infection or left untreated. The mean percentage of infected BMM (G) and the mean *M. tuberculosis*-gfp MFI gated on infected cells (H) determined 5 days after infection and representative histograms are shown (I and J). Differences are significant at *, $P \leq 0.05$; **, $P \leq 0.01$; and ***, $P \leq 0.001$, one-way ANOVA test with Welch's correction.

(Fig. 6E to H). In agreement, *inos* mRNA and nitrite levels in BCG-infected BMM, MGO-treated BMM were restored by incubation with DFO (Fig. S5A and B).

As shown above, DFO and MGO controlled the protein levels of HIF-1 α and HIF-1 activity in BMM; however, *hif1a* mRNA accumulation in *M. tuberculosis*-infected BMM treated with either DFO and/or MGO or left untreated was similar (Fig. 6I).

HIF-1 mediates the activation of the glycolytic pathway and decreased flux through the tricarboxylic acid cycle, to decrease mitochondrial reactive oxygen species (ROS) production (37). BMM were loaded with MitoTracker Green or MitoTracker Deep Red probes to detect mitochondrial content and mitochondrial membrane potential, respectively. We found that the mitochondrial content and potential membrane were increased after mycobacterial infection of BMM. The levels of Mitotracker Green and Deep red were reduced in mycobacteria-infected BMM treated with DFO as well as those treated with MGO and DFO, in comparison to untreated, infected controls or to infected BMM incubated with MGO (Fig. 6J to L).

The incubation with DFO also reduced the percentage of *M. tuberculosis*-infected BMM that were stimulated with IFN- γ and treated with MGO. The percentage of IFN- γ -activated, DFO- and MGO-treated-infected BMM was similar to that of IFN- γ -stimulated (DFO- and MGO-untreated) BMM (Fig. 6M and N).

IFN- γ stimulated *M. tuberculosis*-infected BMM showed a higher level of nitrite in the

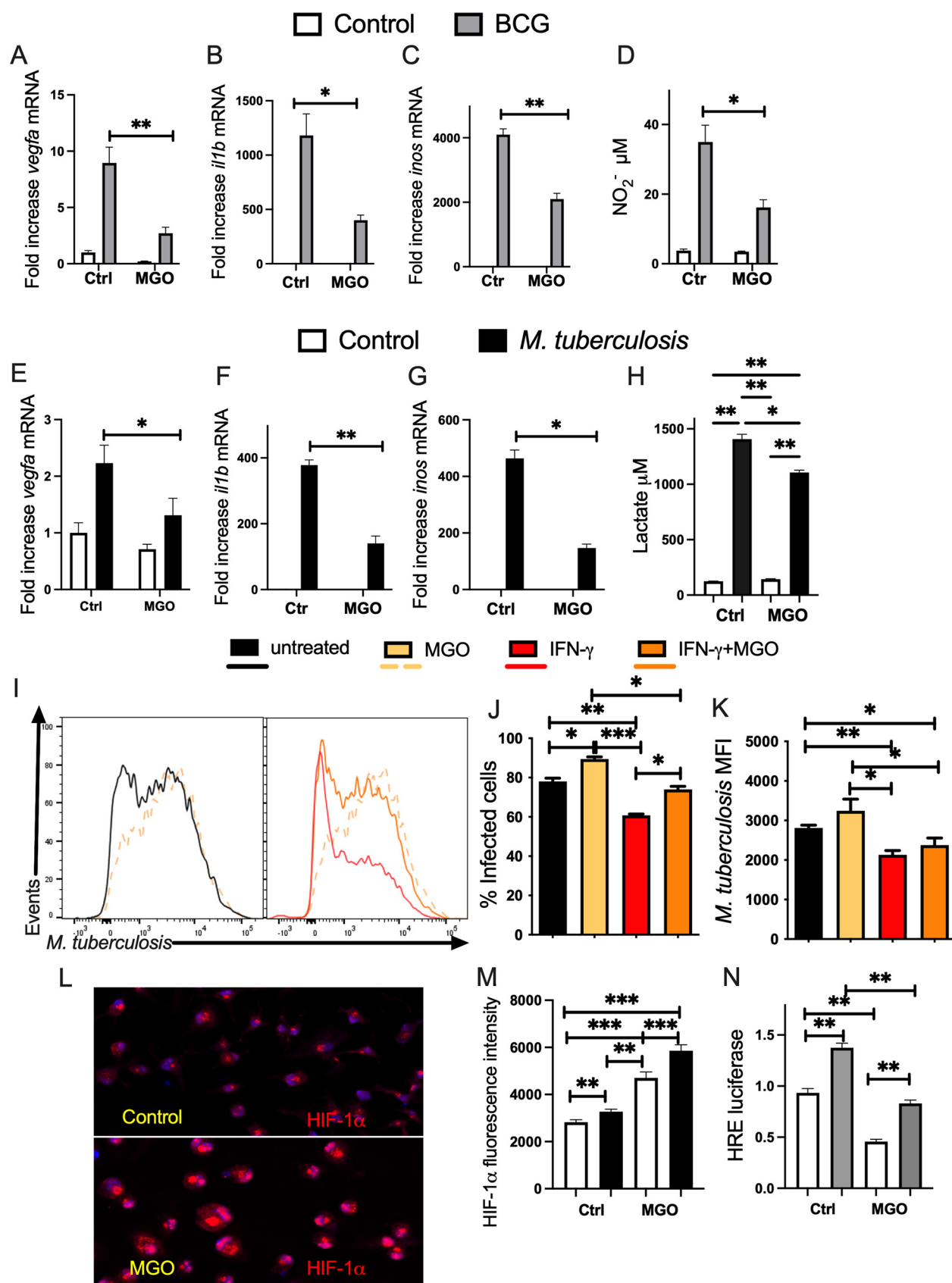


FIG 4 Treatment with methylglyoxal (MGO) hampers control of *M. tuberculosis* infection and HIF-1-regulated responses of BMM A-C.BMM were incubated with 200 μM MGO and infected with BCG 4 h after. (A to C) The mean fold increase of *vegfa* (A), *il1b* (B), and *inos* (C) mRNA was (Continued on next page)

supernatant compared to nonstimulated-infected BMM (Fig. 6O). The addition of DFO further increased nitrite levels whereas incubation with MGO diminished nitrite concentration by IFN- γ -activated-infected BMM. The nitrite levels in IFN- γ -activated *M. tuberculosis*-infected BMM treated with MGO and DFO were similar to those of IFN- γ -stimulated, -untreated BMM (Fig. 6O).

DFO reverts the high-glucose-impaired HIF-1-mediated responses and *M. tuberculosis* control by BMM. Next, the effect of DFO on BCG-infected BMM incubated at normal or high-glucose levels was evaluated. We found that the reduced *vegfa*, *il1b*, and *inos* mRNA levels in infected BMM cultured in high-glucose concentrations were restored by coincubation with DFO (Fig. 7A to C), while levels of *tnf* were not altered by the treatments (Fig. 7D).

Whether high-glucose concentrations could alter the control of *M. tuberculosis* growth in BMM was then tested. BMM were infected with *M. tuberculosis* at an MOI 0.5 and MOI 2, and DFO was added 4 h after. BMM cultured in normal or high-glucose levels showed similar uptake of *M. tuberculosis* at 4 h after infection (Fig. 7E and F). The BMM cultured in 25 mM glucose showed higher titers of *M. tuberculosis* than BMM cultured in 5 mM glucose. DFO treatment reduced *M. tuberculosis* bacterial numbers at 72 h after infection compared to those in nontreated BMM. Coincubation with DFO also reduced *M. tuberculosis* titers in 25 mM glucose-treated BMM (Fig. 7E and F).

To confirm that HIF-1 is a main transcriptional controller of inflammatory and metabolic genes during mycobacterial infection, the responses of *Hif1a*-deficient (*Hif1a^{fl/fl} lysm cre*) and control BMM to infection were studied. *Vegfa*, *glut-1*, *pdk1*, and *ldha* mRNA were reduced in BCG-infected and noninfected *Hif1a^{fl/fl} lysm cre* BMM compared to controls (Fig. 7G to J). Moreover, *il1b* and *inos* mRNA levels were also diminished in *hif1a*-deficient BMM (Fig. 7K and L). The levels of metabolic and immune transcripts in mycobacteria-infected *Hif1a^{fl/fl} lysm cre* BMM incubated in high and normal glucose conditions were similar (Fig. 7G to L). As a control, *Hif1a* mRNA levels were reduced after infection of *Hif1a^{fl/fl} lysm cre* BMM (Fig. 7M). Altogether, this suggests that loss of HIF-1 abrogates the metabolic and immune responses to infection with mycobacteria.

DISCUSSION

Here, we showed that chemical stabilization of HIF-1 by DFO increased the metabolic and immune activation and improved bacterial control during *M. tuberculosis* infection *in vitro* and *in vivo*. High-glucose concentration and MGO treatment reduced HIF-1-dependent immunometabolic responses and diminished the intracellular *M. tuberculosis* control in BMM. Moreover, the stabilization or increased transcriptional activation of HIF-1 by DFO restored both BMM activation and the restriction of intracellular bacterial growth in BMM treated with MGO or incubated in high-glucose conditions (Fig. 8).

Specifically, we showed that BMM infected with *M. tuberculosis* or BCG and lungs from *M. tuberculosis*-infected mice had increased levels of HIF-1 α and HIF-1-regulated

FIG 4 Legend (Continued)

measured in triplicate BMM cultures \pm SEM as measured by RT-PCR. Differences are significant at *, $P \leq 0.05$ and **, $P \leq 0.01$, one-way ANOVA with Welch's adjustment. (D) The concentration of nitrite in the supernatants of MGO-treated and/or BCG-infected BMM was measured 72 h after culture. (E to G) BMM incubated with 125 μ M MGO for 4 h and infected with *M. tuberculosis* thereafter. The mean fold increase of *vegfa* (E), *il1b* (F), and *inos* (G) mRNA was measured in triplicate BMM cultures \pm SEM was measured by RT-PCR. Differences between infected groups are significant at *, $P \leq 0.05$ and **, $P \leq 0.01$, one-way ANOVA with Welch's adjustment. (H) The lactate concentration in the supernatants from BMM treated with MGO 4 h before infection with *M. tuberculosis* was measured by lactate dehydrogenase assay. The mean lactate concentration \pm SEM in BMM supernatants 72 h after infection is shown. Differences are significant at *, $P \leq 0.05$ and **, $P \leq 0.01$, one-way ANOVA with Welch's adjustment. (I) A group of BMM was treated with IFN- γ starting 48 h before *M. tuberculosis*-gfp infection. IFN- γ -treated and control BMM were treated with 400 μ M MGO 4 h before infection with *M. tuberculosis*-gfp (MOI 1:1). (I to K) Representative histograms (I), the mean percentage of infected BMM (J), and the MFI of intracellular *M. tuberculosis* (K) quantified 5 days after infection are shown. Differences are significant at *, $P \leq 0.05$; **, $P \leq 0.01$; and ***, $P \leq 0.001$, one-way ANOVA with Welch's correction. (L and M) Representative micrographs (L) of uninfected MGO-treated and control BMM and the mean \pm SEM intensity of HIF-1 α immunolabeling (M) of MGO-treated, uninfected-, or *M. tuberculosis*-infected BMM determined 24 h after infection. Differences are significant at *, $P \leq 0.05$ and ***, $P \leq 0.001$, one-way ANOVA with Welch's adjustment. (N) The relative HRE activity in RAW macrophages treated or not with MGO was evaluated 24 h after BCG infection. The mean relative luciferase levels \pm SEM in triplicate independent cultures are depicted. Differences are significant at **, $P \leq 0.01$, one-way ANOVA with Welch's correction.

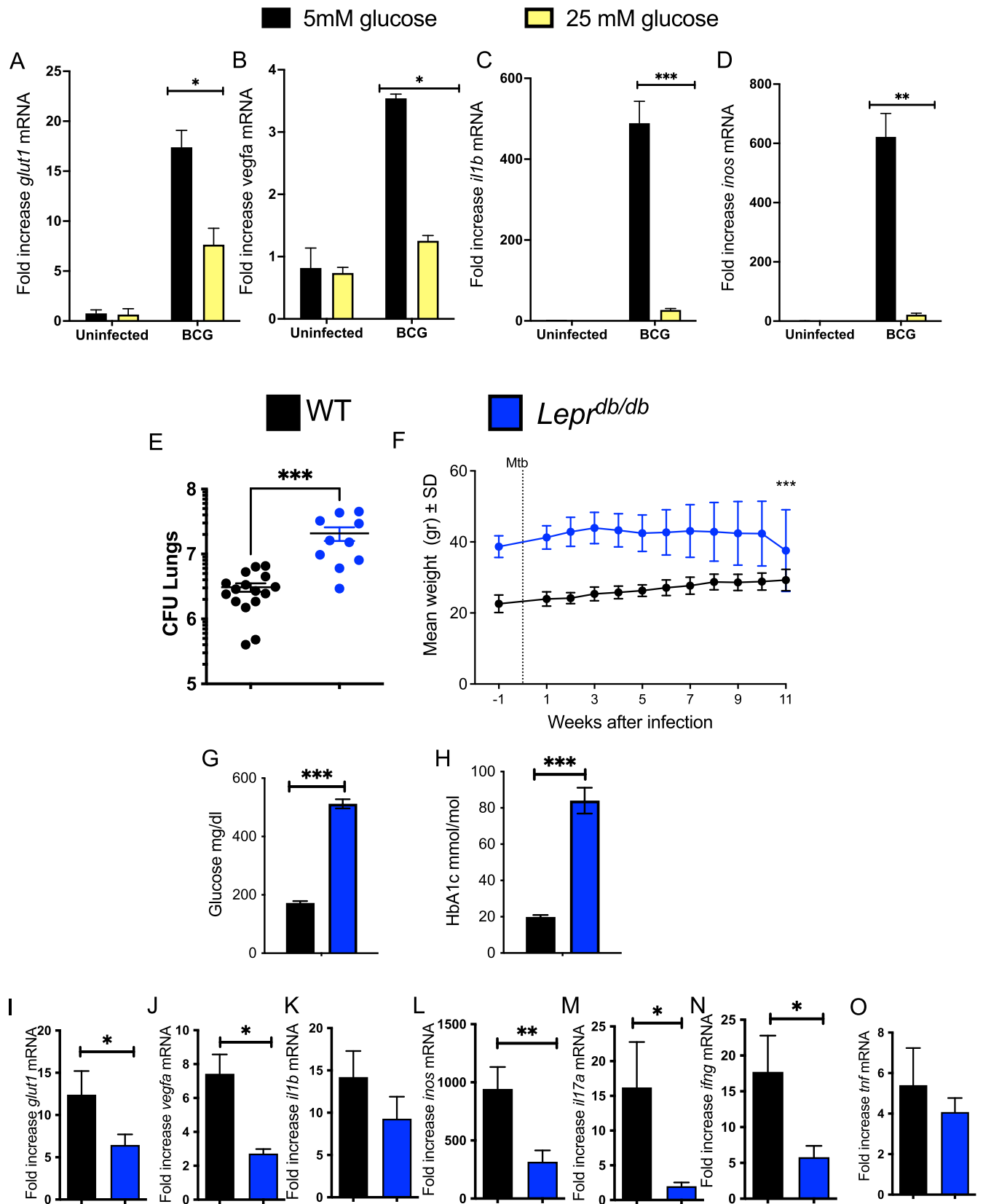


FIG 5 Impaired HIF-1-responses and enhanced susceptibility to *M. tuberculosis* infection in hyperglycemic *Lepr^{db/db}* mice and in high-glucose-level-treated BMM. (A to D) BMM were medium containing 5 mM or 25 mM glucose and infected with BCG 3 days after infection. Total RNA was extracted 24 h after infection and the levels of *glut1* (A), *vegfa* (B), *il1b* (C), and *inos* (D) and *hrpt* were measured by real-time PCR. The mean fold increase of transcript levels in triplicate

(Continued on next page)

immune and metabolic transcripts as well as NO release. HIF-1 expression in immune cells can be triggered by hypoxia but also by inflammation and stimulation by infectious microorganisms in an oxygen-independent manner (38). Bacteria-induced expression of HIF-1 α has been shown in macrophages cultured under normoxic conditions in the presence of different pathogens or innate immune receptor ligands (39, 40), as also shown here for virulent *M. tuberculosis* or the attenuated BCG mycobacterial strains.

The incubation with DFO further increased the HIF-1 levels in BMMs, the glycolytic metabolism, as shown by increased levels of lactate and transcripts for key glycolytic enzyme transcripts, as well as reduced mitochondrial functions. Our data confirm previous results using Seahorse technology, showing that DFO enhances glycolytic metabolism in *M. tuberculosis*-stimulated human macrophages during mitochondrial distress (41). DFO has also been shown to improve the efficiency of antibiotic treatment of BCG-infected macrophages (42). While DFO may display a direct antimycobacterial effect (43), bacterial toxicity was not observed at the DFO concentrations we used. DFO also supported the augmented expression of HIF-regulated inflammatory genes in *M. tuberculosis*-infected BMM. Administration of DFO to uninfected or *M. tuberculosis*-infected mice increased their HIF-1-regulated responses and resulted in a reduction of the levels of *M. tuberculosis* in lungs. The reduction of bacterial load in DFO-treated animals was moderate, supporting the possibility of testing other HIF stabilizers as adjunctive TB treatment or improving DFO delivery. Distinct responses to HIF stabilization in different cell populations or the relatively short half-life of DFO *in vivo* (44) could also explain the moderate protection against *M. tuberculosis* after DFO administration *in vivo*. Instead, BMM incubated with DFO showed an important reduction of intracellular *M. tuberculosis* levels. DFO further reduced bacterial load in IFN- γ -activated BMM, in agreement with an increased NO production. DFO has been indicated to impair HIF-1 α hydroxylation by inhibiting the activity of iron-dependent prolyl hydroxylases (45–47). In addition to HIF-1 α stability, O₂ and iron levels also regulate the transactivation activity of HIF-1 α , which is mediated by factor inhibiting HIF-1 (FIH-1), which hydroxylates an asparagine residue of HIF-1 α and inhibits HIF-1 α activity by limiting recruitment of the coactivator CBP/p300 (48). DFO has been shown to be an effective inhibitor of FIH, promoting full transcriptional activity of HIF-1 (49). Despite the important association with HIF-1 as a target mechanism for DFO, whether other intracellular mechanisms regulated by iron chelation could account for the improved mycobacterial control by DFO cannot be ruled out by our study. For example, the intracellular availability of iron is crucial for bacterial growth and iron regulation via ferropontin and hepcidin might also affect infection control by DFO (50).

Destabilization or functional repression of HIF-1 is the event that transduces hyperglycemia into the loss of the cellular response to hypoxia in DM (30, 48, 51).

MGO, a ubiquitous product of cellular metabolism, is the most significant and highly reactive glycation agent *in vivo* and is considered one of the critical factors in the pathogenesis of diabetic complications (5). The primary source for MGO synthesis in eukaryotic cells is triose phosphates from the glycolytic bypass. As triose phosphates are intermediate products of glycolysis, blood and intracellular glucose levels are determinants of MGO levels. Most of the effects of carbonyl compounds are executed by AGEs, which bind to and alter

FIG 5 Legend (Continued)

cultures \pm SEM is depicted. One out of at least 2 independent experiments is depicted. (E) *Lep^{rd/db}* and control C57BL/6 mice were sacrificed 11 weeks after aerosol infection with *M. tuberculosis*, and CFU (CFU) per lung were assessed. The CFU per organ of individual mice and the median per group at the indicated time points after infection are depicted (median CFU/lung *Lep^{rd/db}*: 20.7·10⁶; WT: 3.08·10⁶). Differences in CFU are significant (***, $P < 0.001$, Mann-Whitney U test). (F) The mean weight \pm SEM of *Lep^{rd/db}* and WT mice during infection with *M. tuberculosis* ($n = 9$ animals per group). Differences between groups were significant at ***, $P \leq 0.001$, two-way ANOVA test. (G and H) The levels of glucose (G) and HbA1c (H) were measured in the plasma of infected WT and *Lep^{rd/db}* mice 11 weeks after infection with *M. tuberculosis* as detailed in Materials and Methods. Differences between WT and *Lep^{rd/db}* groups are significant at ***, $P < 0.001$, unpaired Student's t test. (I to O) Total RNA was extracted from the lungs of *Lep^{rd/db}* and control C57BL/6 mice 11 weeks after aerosol infection with *M. tuberculosis*. The levels of *glut1* (I), *vegfa* (J), *il1b* (K), *inos* (L), *il17a* (M), *ifng* (N), and *tnf* (O) mRNA were determined by real-time PCR. The mean fold increase of mRNA level \pm SEM in 8 mice per group of 1 of 2 independent experiments is depicted. Differences between groups are significant (*, $P < 0.05$; **, $P < 0.01$; ***, $P < 0.001$, unpaired Student's t test with Welch's correction).

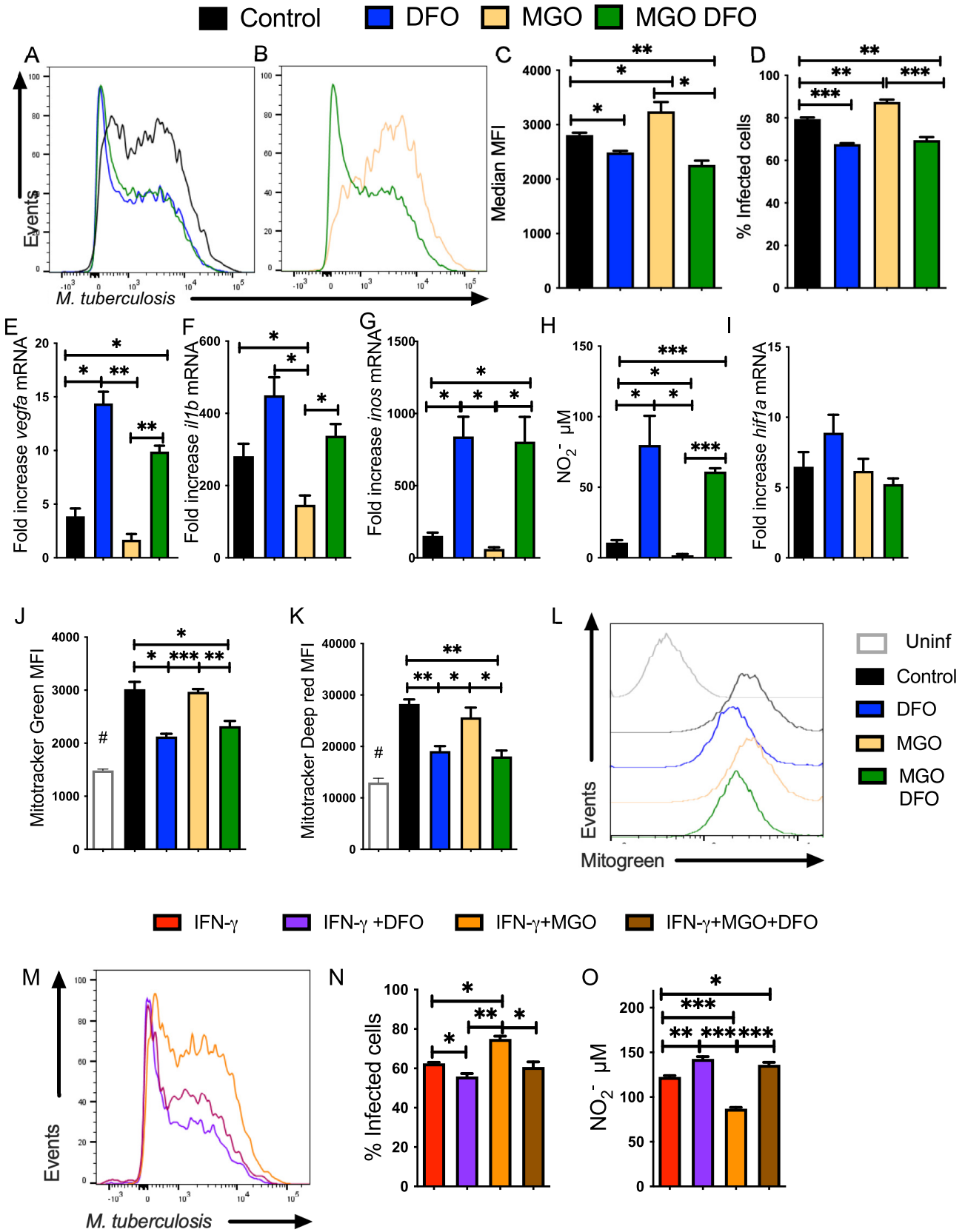


FIG 6 DFO reverts the MGO-hampered HIF-1-mediated responses and the enhanced susceptibility to *M. tuberculosis* infection of BMM. (A to D) A group of BMM cultures were treated with MGO. Four hours later, MGO-treated and control BMM were infected with *M. tuberculosis*-gfp (MOI 1:1). (Continued on next page)

the tertiary structure and function of proteins. Several studies have reported the positive association between plasma carbonyl compounds and AGEs levels in DM patients (52). While MGO has been associated with oxidative and inflammatory responses through the formation of AGEs (52), here we showed that MGO decreases the expression of HIF-1-regulated immunometabolic molecules and impairs the control of *M. tuberculosis* during infection of IFN- γ activated and control BMM. Of interest, MGO did not decrease the levels of HIF-1 α in BMM before or after infection with *M. tuberculosis* but might have inhibited the expression of HIF-1 α -regulated genes by a ROS-mediated modification of p300 (31, 48, 53, 54). In line with this, HIF-1 activity, not stability, has been shown to be impaired in a high-glucose environment due to decreased association of HIF-1 α and its coactivator p300 (30, 55). In agreement, BMM cultured in high-glucose conditions also showed diminished HIF-1-regulated genes and infected BMM cultured in high-glucose levels showed higher intracellular *M. tuberculosis* levels than BMM cultured in normoglycemic conditions.

The leptin receptor-deficient *Lepr^{db/db}* diabetic mice showed increased susceptibility to *M. tuberculosis* infection, confirming previous observations using *Lepr^{db/db}* as well as in leptin-deficient *Lep^{ob/ob}* mice (56, 57). *Lepr^{db/db}* mice showed reduced levels of expression of HIF-1-controlled inflammatory and metabolic genes during infection with *M. tuberculosis*, which associates with the impaired responses of *M. tuberculosis*-infected BMM treated with MGO and high-glucose levels *in vitro*. Direct leptin sensing in immune cells has been shown to be dispensable for immune control of *M. tuberculosis in vivo* (56).

Promoting HIF-1 function with DFO was able to revert the inhibition of immunometabolic responses and the defective intracellular bacterial control by both high-glucose and MGO treatment in control and IFN- γ -activated macrophages. In line with this, maintaining HIF-1 signaling has been shown to prevent DM complications in patients as well as in experimental models (32, 51, 58–61). The deletion of *hif1a* gene in BMM decreased metabolic and inflammatory transcripts as well as metabolites, confirming a nonredundant role of HIF-1 in the activation of these genes that cannot be compensated by HIF-2.

Diabetes increases the risk of several microbial infections, including those by viruses such as Sars-CoV-2, influenza, hepatitis B, and hepatitis C and bacteria such as *Streptococcus pneumoniae*, *Helicobacter pylori*, *Staphylococcus aureus*, *Haemophilus influenzae*, and *Escherichia coli* among others that affect the respiratory tract and the urinary tract or cause soft tissue infections (such as foot infections) (62). The inhibition of HIF-responses in DM may also regulate the risk of acquiring or developing an increased severity of these infections.

Altogether, our results suggest repressed HIF-1-mediated responses in DM as a mechanism underlying the increased risk of developing TB in DM patients. We also show that promoting HIF-1 function with DFO was able to revert the inhibition of

FIG 6 Legend (Continued)

BMM were either treated with 100 μ M DFO or left untreated 4 h after infection. Representative histograms (A and B), the mean *M. tuberculosis*-gfp MFI (C), and the mean percentage of infected BMM (D) at 5 days after infection are shown. Differences are significant at *, $P \leq 0.05$; **, $P \leq 0.01$; and ***, $P \leq 0.001$, one-way ANOVA test with Welch's adjustment. (E to G and I) BMM were incubated with MGO and 1 h after being infected with *M. tuberculosis*. MGO-treated or control BMM were further incubated with DFO 4 h after infection. The mean fold increase of *vegfa* (E), *il1b* (F), *inos* (G), and *hif1a* (I) mRNA was measured in triplicate BMM cultures \pm SEM was measured by RT-PCR. Differences are significant at *, $P \leq 0.05$ and **, $P \leq 0.01$, one-way ANOVA test with Welch's correction. (H) The mean concentration of nitrite \pm SEM in supernatants of MGO and/or DFO-treated, *M. tuberculosis*-infected BMM was measured 72 h after culture. Differences are significant at *, $P \leq 0.05$ and ***, $P \leq 0.001$, one-way, Welch's adjusted, ANOVA test. (J to L) BMM were either treated with MGO 4 h before BCG infection and/or with DFO 4 h after infection. A group of BMM was left uninfected. Forty-eight hours after infection, BMM were incubated with Mito tracker Green (I) or Mito tracker Deep Red (J) for 30 min at 37°C. The mean fluorescence intensity of the different groups ($n = 3$ per group) \pm SEM and representative histograms of Mito Tracker Green-labeled cells (K) are shown. This experiment was repeated three times. Differences are significant at *, $P \leq 0.05$, **, $P \leq 0.01$; and ***, $P \leq 0.001$, one-way Welch's adjusted ANOVA test. #, Differences with the uninfected group are statistically significant. (M and N) BMM was treated with IFN- γ 48 h before infection with *M. tuberculosis*. Further, a group of BMM was treated with MGO 4 h before infection. MGO-treated and control BMM were infected with *M. tuberculosis*-gfp. Four hours after infection, BMM were either treated with 100 μ M DFO or left untreated. Representative histograms (M) and the mean percentage of infected BMM \pm SEM (N) quantified 5 days after infection are shown. Differences are significant at *, $P \leq 0.05$ and **, $P \leq 0.01$, one-way ANOVA test with Welch's correction. (O) The nitrite concentration in supernatants of IFN- γ -activated BMM treated with MGO and/or DFO treated was measured 72 h after infection with *M. tuberculosis*. Differences are significant at *, $P \leq 0.05$; **, $P \leq 0.01$; and ***, $P \leq 0.001$, one-way Welch ANOVA test.

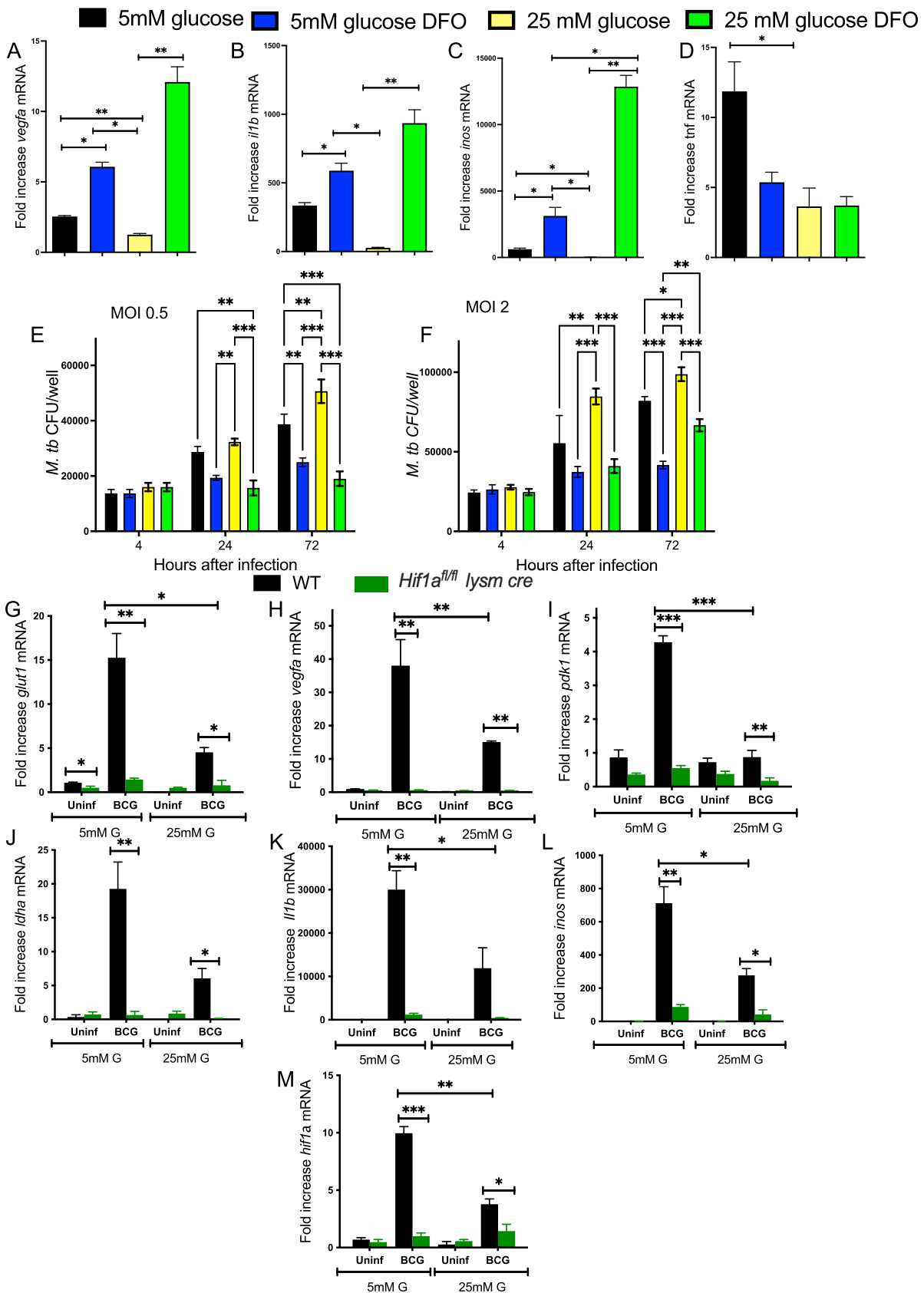


FIG 7 DFO reverts the high-glucose concentration-hampered HIF-1-mediated responses and the enhanced susceptibility to *M. tuberculosis* infection of BMM. (A to D) BMM were cultured in medium containing 5 mM or 25 mM glucose and infected with BCG 3 days (Continued on next page)

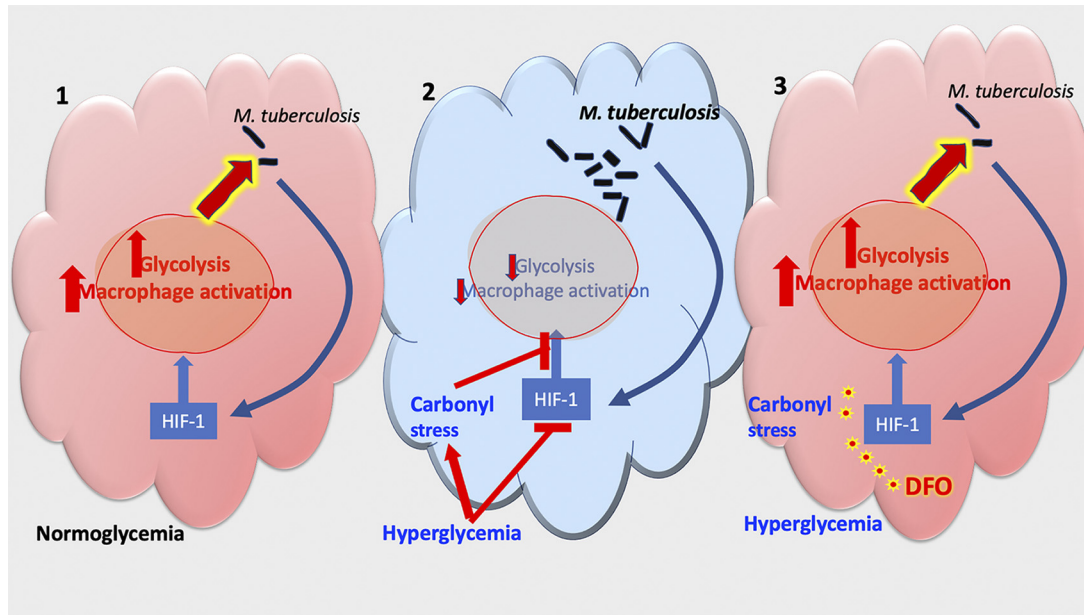


FIG 8 Summary. (1) Infection with *M. tuberculosis* induces the expression of HIF-1-regulated genes after in BMM. These genes mediate the metabolic switch and macrophage activation required to control the intracellular bacterial infection. (2) During DM, high levels of glucose and reactive carbonyl compounds hamper the expression of HIF-1-regulated genes and in turn impair the control of intracellular *M. tuberculosis* in BMM. (3) Treatment with the hypoxia mimic deferoxamine (DFO) increased immunometabolic responses in infected BMMs and in the lungs of *M. tuberculosis*-infected mice. DFO treatment reduced the *M. tuberculosis* titers in BMM treated or not with IFN- γ . Treatment with DFO restored HIF-1-regulated responses to infection and improved *M. tuberculosis* control in MGO and high-glucose-treated BMM.

immunometabolic responses and the defective intracellular bacterial control driven by both high-glucose and MGO treatment in control and IFN- γ activated macrophages, constituting a rationale for the design of adjunctive TB therapy in TB/DM comorbidity.

MATERIALS AND METHODS

Ethics statement. The animals were housed and handled at Astrid Fagreu Laboratory, Karolinska Institutet, Stockholm, according to directives and guidelines of the Swedish Board of Agriculture, the Swedish Animal Protection Agency, and the Karolinska Institute (djurskyddslagen 1988:534; djurskyddsförordningen 1988:539; and djurskyddsmyndigheten DFS 2004:4). The study was performed under approval of the Stockholm North Ethical Committee on Animal Experiments permits no. N128/16. Animals were housed under specific pathogen-free conditions.

Mice. Six-week-old BKS(D)-*Leprdb*/JOrI Rj (*Lepr^{db/db}*) obese leptin receptor-deficient mice and C57BL/6 mice were purchased from Janvier (Le Genest St. Isle, France).

All animals used in this study were males between 8 to 20 weeks of age. The animals were housed in groups (three or five) and given free access to food and water.

The mice were under weekly follow-up for body weight and blood glucose. All procedures were performed in a biosafety level III animal facility.

Macrophages from *Hif1a^{fl/fl} Lysm cre* mice were used for *in vitro* experiments. *Hif1a^{fl/fl}* mice with a loxP-targeted deletion of the *hif1a* and the *vhl* gene (19, 63) were crossed with *Lysm cre* transgenic animals in which cre expression is driven by the lysozyme M promoter (64), allowing the deletion of the transcription factor in the myeloid lineage.

FIG 7 Legend (Continued)

after. DFO was added 4 h after infection in indicated groups. Total RNA was extracted 24 h after infection and the levels of *vegfa* (A), *il1b* (B), *inos* (C), and *tnf* (D) mRNA in triplicate independent cultures were measured by real-time PCR. The mean fold increase of transcript levels \pm SEM is depicted. Differences between groups are significant at *, $P \leq 0.05$; **, $P \leq 0.01$; and ***, $P \leq 0.001$, one-way ANOVA test with Welch's correction. (E and F) BMM were incubated with 5 mM or 25 mM glucose 3 days before infection with *M. tuberculosis* at MOI 0.5 (E) or 2:1 (F). BMM were treated with 100 μ M DFO 4 h after the infection. The CFU in cell lysates at the indicated time points after infection was determined. The mean CFU \pm SEM in triplicate independent cultures per condition is shown. Differences between groups are significant at **, $P \leq 0.05$ and **, $P \leq 0.01$, one-way ANOVA test with Welch's correction. (G to M) *Hif1a^{fl/fl} lysm cre* and WT BMM were infected with BCG at an MOI 5:1. Total RNA was extracted 24 h after infection and the levels of *glut1* (G), *vegfa* (H), *pdk1* (I), *ldha* (J), *il1b* (K), *inos* (L), and *hif1a* (M) mRNA in triplicate independent cultures were in either 5 mM or 25 mM glucose measured by real-time PCR. The mean fold increase of transcript levels in triplicate independent cultures \pm SEM is depicted. Differences are significant at *, $P \leq 0.05$; **, $P \leq 0.01$; and ***, $P \leq 0.001$, one-way ANOVA test with Welch's correction.

Reagents. Deferoxamine (DFO), 2-deoxyglucose (2-DG), and D-glucose (Sigma-Aldrich, St. Louis, MO) were used at indicated concentrations for *in vitro* and *in vivo* experiments. DFO was diluted in PBS and freshly prepared before inoculation. Mice in the DFO group were treated i.p. with a 400-mg/kg dose every other day starting 1 day before infection and during 3 months of *M. tuberculosis* infection until 1 day before take down. Similar DFO treatment of mice schemes was previously reported to lack toxicity (65).

Infection of mice with *M. tuberculosis*. Mice were infected with 200 CFU *M. tuberculosis* Harlingen strain using a nose-only aerosol exposure unit (In-tox Products, NM, USA). The dose indicates the bacteria recovered in lungs 24 h after infection. A 15-ml suspension of 1×10^6 *M. tuberculosis* per ml was loaded into a nebulizer, and animals inhaled the bacteria aerosol for 20 min. Mice were sacrificed at indicated time points after infection and bacteria from organ lysates was plated and quantified on Middlebrook 7H11 agar containing 10% enrichment of oleic acid, albumin, dextrose, catalase, 5 μ g amphotericin B per ml, and 8 μ g/ml polymyxin B grown for 3 weeks at 37°C.

Measurement of blood glucose, HbA1c, triglycerides, and cholesterol. A quantitative determination of cholesterol, triglycerides, and glucose levels was determined in 10 μ l tail vein blood using the Multicare-in device (Balerna, Switzerland). Blood glucose was measured every week, while triglycerides and cholesterol were measured every 2 weeks until mice take down.

Glycated hemoglobin (HbA1c) was measured using the DCA Vantage Analyzer (Siemens) device in 1 μ l tail vein blood. HbA1c measurements were done before and after infection with *M. tuberculosis*.

Generation of mouse bone marrow-derived macrophages. Bone marrow cells were flushed from tibia and femurs with PBS, filtered through a 70- μ m cell strainer, resuspended in DMEM supplemented with 10% FCS and 30% L929 cell-conditioned medium (as a source of macrophage-colony-stimulating factor), and incubated for 6 days at 37°C, 5% CO₂. Bone marrow-derived macrophage (BMM) cultures were then washed with PBS and detached with 1% trypsin, and $5 \cdot 10^5$ cells were seeded to each well at (using 24-well plates). BMM were further incubated for 24 h at 37°C before infections or treatment with diverse compounds. Confirming previous data (66), BMM were F4/80⁺, CD11b⁺.

Infection of BMM with mycobacteria. *M. tuberculosis* Harlingen or H37Rv carrying the green fluorescent protein (GFP)-encoding pFPV2 plasmid were grown in Middlebrook 7H9 (Difco, Detroit, MI) supplemented with albumin, dextrose, and catalase and quantified by densitometry. BMM were infected with sonicated bacteria at a multiplicity of infection (MOI) of 0.5 and 2. After 4 h, cells were washed twice with PBS to remove extracellular bacteria and further incubated for 1 to 5 days. At these time points, BMM were lysed with 0.1% Triton X, and the suspensions were plated on Difco Middlebrook 7H11 agar enriched with oleic acid-albumin-dextrose catalase supplement (BD) to quantify *M. tuberculosis* CFU.

Alternatively, BMM were infected as described above at different MOI (0.3, 1, or 3) with *M. tuberculosis*-GFP (67). The infected BMM were detached using trypsin-EDTA at different times after infection. Cell suspensions were incubated with live/dead stain (LIVE/DEAD Fixable Yellow Dead Cell Stain, Invitrogen), washed with FACS buffer (PBS containing 0.5% FCS and 0.5 mM EDTA), and fixed with 4% formaldehyde (Sigma-Aldrich) at room temperature (RT) for 10 min. Data were acquired on a LSRII flow cytometer and analyzed with FlowJo software (Tree star Inc., Ashland, OR). Cells in the mononuclear gate were $\geq 95\%$ live, and $\geq 95\%$ of live cells were CD11b⁺, F4/80⁺ (see the gating strategy in Fig. S6).

Immunofluorescent labeling of HIF-1 α . HIF-1 α was labeled in 4% PFA-fixed *M. tuberculosis*-infected or uninfected BMM treated or not with DFO or MGO. Cells were stained with anti-HIF-1 α (1:100; clone HIF-1 α 67; BD) antibody in 1:1 ratio of 1 \times PBS with 0.1% Tween 20 (PBS-T) and 5% BSA and 5% donkey serum in PBS. Cells were washed with 1 \times PBS-T and further incubated with secondary Alexa Fluor 488-conjugated goat anti-mouse IgG antibody (Invitrogen) 1:100 for 1 h at room temperature, followed by staining with DAPI for 15 min and washed and mounted in Fluoromount G (Southern Biotech). Slides were analyzed with a Leica epi-fluorescence microscope using 40 \times objective. Fluorescence intensity was quantified in three to five random fields of view per coverslip with the Cell Profiler software pipeline. Briefly, DAPI channel was segmented using the "IdentifyPrimaryObjects" function to detect nuclei, and Rhodamine Red intensity was then measured.

Mitochondrial content and potential. *M. tuberculosis*-infected BMM were detached and stained with 150 nM MitoTracker Green fluorescent dye or with MitoTracker Deep Red (Thermo Fisher Scientific) for 30 min 37°C. The far red-fluorescent MitoTracker Deep Red was used to measure the mitochondrial membrane potential while Mitotracker green labeling was used as an estimation of the mitochondrial mass. Fluorescence-labeled mitochondria in BMM were fixed with subjected after fixation to FACS analysis.

L-lactate assay. Lactate accumulation in BMM supernatants was measured using the L-lactate assay kit (Cayman Chemicals) as described in the manufacturer's protocol. In the assay, lactate dehydrogenase catalyzes the oxidation of lactate to pyruvate, along with the concomitant reduction of NAD⁺ to NADH. NADH reacts with the fluorescent substrate to yield a highly fluorescent product. The fluorescent product was analyzed after a 15-min RT incubation with BMM supernatants with an excitation wavelength of 540 nm.

Nitrite. To analyze the concentration of the stable oxidation products of nitric oxide (NO) in the BMM supernatants, the total concentration of nitrite and nitrate was calculated by performing the Griess reaction as previously described (68). Briefly, 100 μ l of 1% (wt/vol) sulfanilamide in 5% phosphoric acid followed by 100 μ l 0.1% (wt/vol) *N*-(1-naphthyl) ethylenediamine HCl was added to 50 μ l of samples. After incubation for 10 min at RT, the absorbance was read at 540 nm.

Real-time PCR. Total RNA was extracted from lung samples or culture cells using TRIzol (Sigma-Aldrich) and cDNA was obtained by reverse transcription. Transcripts were quantified by real-time PCR as previously described (69). The relative number of transcripts was calculated using the $2^{-\Delta\Delta CT}$ method. These values were then used to calculate the relative expression of mRNA in the different

conditions (infection and/or treatment) used in tissues and cells. Transcripts were quantified using *hprt* as a control housekeeping gene to calculate the ΔCT values for individual samples.

The primer sequences for sense (S) and antisense (AS) were as follows: *hprt* (S) 5'-CCCAGCGTCGT GATTAGC-3' and *hprt* (AS) 5'-GGAATAAACACTTTTTCCAAATCC-3'; *inos* (S) 5'-CAGCTGGGCTGTACAAACCTT-3' and *inos* (AS) 5'-CATTGGAAGTGAAGCGTTTCG-3'; *il1b* (S) 5'-TGGTGTGTGACGTTCCATT-3' and *il1b* (AS) 5'-CAGCAGAGGCTTTTTTTGTTG-3'; *tnf* (S) 5'-GGCTGCCCGACTACGT-3' and *tnf* (AS) 5'-GACTTTCTCTGGTAT GAGATAGCAA-3'; *ifng* (S) 5'-GCT TIG CAG CTC TTC CTC AT-3' and *ifng* (AS) 5'-CAC ATC TAT GCC ACT TGA GTT AAA ATA GT-3'; *glut1* (S) 5'-AAGTCCAGGAGGATATTAG-3' and *glut1* (AS) 5'-CTACAGTGTGGAGATA GGAG-3'; *vegfa* (S) 5'-TAGAGTACATACTTCAAGCCG-3' and *vegfa* (AS) 5'-TCTTTCTTTGGTCTGCATTC-3'; *hif1a* (S) 5'-CGATGACACAGAACTGAAG-3' and *hif1a* (AS) 5'-GAAGGTAAGGAGACATTGC-3'; *pdk1* (S) 5'-GAAGCA GTTCTGGACTTCG -3' and *pdk1* (AS) 5'-CCAATTTGCACCAGCTGTA -3'; and *ldha* (S) 5'-TGGCAGACTTGGCT GACAG-3' and *ldha* (AS) 5'-ACCTTCACAACATCCGAGATTC-3'.

HRE-driven luciferase promoter assay. HIF-1 activity was determined by an HRE-driven luciferase reporter assay as described previously (58). Briefly RAW macrophages were transiently transfected with HRE-luciferase reporter gene plasmid (pT81/HRE-luc) using Lipofectamine (Thermo Fisher Scientific) according to the manufacturer's instructions. Renilla luciferase vector, which provides constitutive expression, was cotransfected with HRE-luciferase plasmid and used as an internal control. Transfected cells were infected or not with BCG (24 h after transfection) and cultured in media containing either DFO or MGO for 24 h. The macrophages were harvested, and luciferase activity was measured using the Dual Luciferase Assay System (Promega) on the GloMax Luminometer (Promega) according to the manufacturer's instructions. HRE-driven firefly luciferase activity was normalized to Renilla luciferase activity and expressed as relative luciferase activity.

Statistical analysis. All *in vitro* assays were performed at least in biological triplicates and were independently twice or more. Differences in bacterial counts in the lungs of infected mice were calculated using the nonparametric Mann-Whitney's U test. Differences in cytokine transcripts, lactate, nitrites, and CFU were measured by unpaired Student's *t* test considering unequal variances (Welch's test) and by one-way ANOVA using Welch's adjustment when comparing three or more groups. In this case, a two-way ANOVA was used when more than two parameters were analyzed (i.e., time after infection and treatments). Multiple comparisons were corrected by the false discovery rate method. The statistical tests were performed using the Prism software (GraphPad, La Jolla, CA).

SUPPLEMENTAL MATERIAL

Supplemental material is available online only.

FIG S1, EPS file, 2 MB.

FIG S2, EPS file, 0.4 MB.

FIG S3, TIF file, 0.7 MB.

FIG S4, EPS file, 0.3 MB.

FIG S5, EPS file, 0.1 MB.

FIG S6, JPG file, 0.2 MB.

ACKNOWLEDGMENTS

We thank the expert help of the staff of the Astrid Fagreu's animal house, Department of Comparative Medicine, Karolinska Institutet, and Juan Basile at the FACS facility Karolinska Institutet. We thank Sophie Essay and Asma Araba (Karolinska Institutet) for assistance in the studies. We thank Randall Johnsson (University of Cambridge and Karolinska Institutet) for gently providing *Hif1a*^{fl/fl} mice.

This study was supported by the Swedish Heart and Lung foundation 2018-20/20170491, the Swedish Research Council 2019-01691 and 2019-04725, the Swedish Institute for Internationalization of Research (STINT) 4-1796/2014, the European Community H2020 EMITB (grant number 643558), the Chinese Scholarship Council, the Swedish International Development Agency (SIDA) and the Karolinska Institutet. The funders had no role in study design, data collection and interpretation, or the decision to submit the work for publication.

We declare that the research was conducted in the absence of any commercial or financial relationships that could be construed as a potential conflict of interest.

REFERENCES

1. WHO. 2019. Global tuberculosis report 2019. Geneva, Switzerland: World Health Organization.
2. Cohen SB, Gern BH, Delahaye JL, Adams KN, Plumlee CR, Winkler JK, Sherman DR, Gerner MY, Urdahl KB. 2018. Alveolar macrophages provide an early mycobacterium tuberculosis niche and initiate dissemination. *Cell Host Microbe* 24:439–446.e4. <https://doi.org/10.1016/j.chom.2018.08.001>.
3. Brownlee M. 2005. The pathobiology of diabetic complications: a unifying mechanism. *Diabetes* 54:1615–1625. <https://doi.org/10.2337/diabetes.54.6.1615>.

4. Ramasamy R, Yan SF, Schmidt AM. 2006. Methylglyoxal comes of AGE. *Cell* 124:258–260. <https://doi.org/10.1016/j.cell.2006.01.002>.
5. Schalkwijk CG, Stehouwer CDA. 2020. Methylglyoxal, a highly reactive dicarbonyl compound, in diabetes, its vascular complications, and other age-related diseases. *Physiol Rev* 100:407–461. <https://doi.org/10.1152/physrev.00001.2019>.
6. Jeon CY, Murray MB. 2008. Diabetes mellitus increases the risk of active tuberculosis: a systematic review of 13 observational studies. *PLoS Med* 5:e152. <https://doi.org/10.1371/journal.pmed.0050152>.
7. Dooley KE, Chaisson RE. 2009. Tuberculosis and diabetes mellitus: convergence of two epidemics. *Lancet Infect Dis* 9:737–746. [https://doi.org/10.1016/S1473-3099\(09\)70282-8](https://doi.org/10.1016/S1473-3099(09)70282-8).
8. Lonnroth K, Castro KG, Chakaya JM, Chauhan LS, Floyd K, Glaziou P, Raviglione MC. 2010. Tuberculosis control and elimination 2010–50: cure, care, and social development. *Lancet* 375:1814–1829. [https://doi.org/10.1016/S0140-6736\(10\)60483-7](https://doi.org/10.1016/S0140-6736(10)60483-7).
9. Baker MA, Harries AD, Jeon CY, Hart JE, Kapur A, Lonnroth K, Ottmani SE, Goonesekera SD, Murray MB. 2011. The impact of diabetes on tuberculosis treatment outcomes: a systematic review. *BMC Med* 9:81. <https://doi.org/10.1186/1741-7015-9-81>.
10. Jeon CY, Harries AD, Baker MA, Hart JE, Kapur A, Lonnroth K, Ottmani SE, Goonesekera S, Murray MB. 2010. Bi-directional screening for tuberculosis and diabetes: a systematic review. *Trop Med Int Health* 15:1300–1314. <https://doi.org/10.1111/j.1365-3156.2010.02632.x>.
11. Martinez N, Kornfeld H. 2014. Diabetes and immunity to tuberculosis. *Eur J Immunol* 44:617–626. <https://doi.org/10.1002/eji.201344301>.
12. Kallio PJ, Wilson WJ, O'Brien S, Makino Y, Poellinger L. 1999. Regulation of the hypoxia-inducible transcription factor 1alpha by the ubiquitin-proteasome pathway. *J Biol Chem* 274:6519–6525. <https://doi.org/10.1074/jbc.274.10.6519>.
13. Bruck RK, McKnight SL. 2001. A conserved family of prolyl-4-hydroxylases that modify HIF. *Science* 294:1337–1340. <https://doi.org/10.1126/science.1066373>.
14. Epstein AC, Gleadle JM, McNeill LA, Hewitson KS, O'Rourke J, Mole DR, Mukherji M, Metzen E, Wilson MI, Dhanda A, Tian YM, Masson N, Hamilton DL, Jaakkola P, Barstead R, Hodgkin J, Maxwell PH, Pugh CW, Schofield CJ, Ratcliffe PJ. 2001. C. elegans EGL-9 and mammalian homologs define a family of dioxygenases that regulate HIF by prolyl hydroxylation. *Cell* 107:43–54. [https://doi.org/10.1016/S0092-8674\(01\)00507-4](https://doi.org/10.1016/S0092-8674(01)00507-4).
15. Maxwell PH, Wiesener MS, Chang GW, Clifford SC, Vaux EC, Cockman ME, Wykoff CC, Pugh CW, Maher ER, Ratcliffe PJ. 1999. The tumour suppressor protein VHL targets hypoxia-inducible factors for oxygen-dependent proteolysis. *Nature* 399:271–275. <https://doi.org/10.1038/20459>.
16. Kallio PJ, Okamoto K, O'Brien S, Carrero P, Makino Y, Tanaka H, Poellinger L. 1998. Signal transduction in hypoxic cells: inducible nuclear translocation and recruitment of the CBP/p300 coactivator by the hypoxia-inducible factor-1alpha. *EMBO J* 17:6573–6586. <https://doi.org/10.1093/emboj/17.22.6573>.
17. Haluszczak C, Akue AD, Hamilton SE, Johnson LD, Pujanauski L, Teodorovic L, Jameson SC, Kedl RM. 2009. The antigen-specific CD8+ T cell repertoire in unimmunized mice includes memory phenotype cells bearing markers of homeostatic expansion. *J Exp Med* 206:435–448. <https://doi.org/10.1084/jem.20081829>.
18. Carroll VA, Ashcroft M. 2006. Role of hypoxia-inducible factor (HIF)-1alpha versus HIF-2alpha in the regulation of HIF target genes in response to hypoxia, insulin-like growth factor-I, or loss of von Hippel-Lindau function: implications for targeting the HIF pathway. *Cancer Res* 66:6264–6270. <https://doi.org/10.1158/0008-5472.CAN-05-2519>.
19. Cramer T, Yamanishi Y, Clausen BE, Forster I, Pawlinski R, Mackman N, Haase VH, Jaenisch R, Corr M, Nizet V, Firestein GS, Gerber HP, Ferrara N, Johnson RS. 2003. HIF-1alpha is essential for myeloid cell-mediated inflammation. *Cell* 112:645–657. [https://doi.org/10.1016/S0092-8674\(03\)00154-5](https://doi.org/10.1016/S0092-8674(03)00154-5).
20. Tannahill GM, Curtis AM, Adamik J, Palsson-McDermott EM, McGettrick AF, Goel G, Frezza C, Bernard NJ, Kelly B, Foley NH, Zheng L, Gardet A, Tong Z, Jany SS, Corr SC, Haneke M, Caffrey BE, Pierce K, Walmsley S, Beasley FC, Cummins E, Nizet V, Whyte M, Taylor CT, Lin H, Masters SL, Gottlieb E, Kelly VP, Clish C, Auron PE, Xavier RJ, O'Neill LAJ. 2013. Succinate is an inflammatory signal that induces IL-1beta through HIF-1alpha. *Nature* 496:238–242. <https://doi.org/10.1038/nature11986>.
21. Ogryzko NV, Lewis A, Wilson HL, Meijer AH, Renshaw SA, Elks PM. 2019. Hif-1alpha-induced expression of Il-1beta protects against mycobacterial infection in zebrafish. *J Immunol* 202:494–502. <https://doi.org/10.4049/jimmunol.1801139>.
22. Cooper AM. 2009. Cell-mediated immune responses in tuberculosis. *Annu Rev Immunol* 27:393–422. <https://doi.org/10.1146/annurev.immunol.021908.132703>.
23. Belton M, Brilha S, Manavaki R, Mauri F, Nijran K, Hong YT, Patel NH, Dembek M, Tezera L, Green J, Moores R, Aigbirio F, Al-Nahhas A, Fryer TD, Elkington PT, Friedland JS. 2016. Hypoxia and tissue destruction in pulmonary TB. *Thorax* 71:1145–1153. <https://doi.org/10.1136/thoraxjnl-2015-207402>.
24. Shi L, Salamon H, Eugenin EA, Pine R, Cooper A, Gennaro ML. 2015. Infection with Mycobacterium tuberculosis induces the Warburg effect in mouse lungs. *Sci Rep* 5:18176. <https://doi.org/10.1038/srep18176>.
25. Braverman J, Sogi KM, Benjamin D, Nomura DK, Stanley SA. 2016. HIF-1alpha is an essential mediator of IFN-gamma-dependent immunity to Mycobacterium tuberculosis. *J Immunol* 197:1287–1297. <https://doi.org/10.4049/jimmunol.1600266>.
26. Casanova JL, Abel L. 2002. Genetic dissection of immunity to mycobacteria: the human model. *Annu Rev Immunol* 20:581–620. <https://doi.org/10.1146/annurev.immunol.20.081501.125851>.
27. Mogues T, Goodrich ME, Ryan L, LaCourse R, North RJ. 2001. The relative importance of T cell subsets in immunity and immunopathology of airborne Mycobacterium tuberculosis infection in mice. *J Exp Med* 193:271–280. <https://doi.org/10.1084/jem.193.3.271>.
28. Cooper AM, Dalton DK, Stewart TA, Griffin JP, Russell DG, Orme IM. 1993. Disseminated tuberculosis in interferon gamma gene-disrupted mice. *J Exp Med* 178:2243–2247. <https://doi.org/10.1084/jem.178.6.2243>.
29. Osada-Oka M, Goda N, Saiga H, Yamamoto M, Takeda K, Ozeki Y, Yamaguchi T, Soga T, Tateishi Y, Miura K, Okuzaki D, Kobayashi K, Matsumoto S. 2019. Metabolic adaptation to glycolysis is a basic defense mechanism of macrophages for Mycobacterium tuberculosis infection. *Int Immunol* 31:781–793. <https://doi.org/10.1093/intimm/dxz048>.
30. Catrina SB, Okamoto K, Pereira T, Brismar K, Poellinger L. 2004. Hyperglycemia regulates hypoxia-inducible factor-1alpha protein stability and function. *Diabetes* 53:3226–3232. <https://doi.org/10.2337/diabetes.53.12.3226>.
31. Thangarajah H, Yao D, Chang EI, Shi Y, Zajayeri L, Vial IN, Galiano RD, Du XL, Grogan R, Galvez MG, Januszky M, Brownlee M, Gurtner GC. 2009. The molecular basis for impaired hypoxia-induced VEGF expression in diabetic tissues. *Proc Natl Acad Sci U S A* 106:13505–13510. <https://doi.org/10.1073/pnas.0906670106>.
32. Botusan IR, Sunkari VG, Savu O, Catrina AI, Grunler J, Lindberg S, Pereira T, Yla-Herttuala S, Poellinger L, Brismar K, Catrina SB. 2008. Stabilization of HIF-1alpha is critical to improve wound healing in diabetic mice. *Proc Natl Acad Sci U S A* 105:19426–19431. <https://doi.org/10.1073/pnas.0805230105>.
33. Takeda N, O'Dea EL, Doedens A, Kim JW, Weidemann A, Stockmann C, Asagiri M, Simon MC, Hoffmann A, Johnson RS. 2010. Differential activation and antagonistic function of HIF-1alpha isoforms in macrophages are essential for NO homeostasis. *Genes Dev* 24:491–501. <https://doi.org/10.1101/gad.1881410>.
34. An WG, Kanekal M, Simon MC, Maltepe E, Blagosklonny MV, Neckers LM. 1998. Stabilization of wild-type p53 by hypoxia-inducible factor 1alpha. *Nature* 392:405–408. <https://doi.org/10.1038/32925>.
35. Ramachandra Bhat L, Vedantham S, Krishnan UM, Rayappan JBB. 2019. Methylglyoxal—an emerging biomarker for diabetes mellitus diagnosis and its detection methods. *Biosens Bioelectron* 133:107–124. <https://doi.org/10.1016/j.bios.2019.03.010>.
36. Kobayashi K, Forte TM, Taniguchi S, Ishida BY, Oka K, Chan L. 2000. The db/db mouse, a model for diabetic dyslipidemia: molecular characterization and effects of Western diet feeding. *Metabolism* 49:22–31. [https://doi.org/10.1016/S0026-0495\(00\)90588-2](https://doi.org/10.1016/S0026-0495(00)90588-2).
37. Semenza GL. 2017. Hypoxia-inducible factors: coupling glucose metabolism and redox regulation with induction of the breast cancer stem cell phenotype. *EMBO J* 36:252–259. <https://doi.org/10.15252/emboj.201695204>.
38. Palazon A, Goldrath AW, Nizet V, Johnson RS. 2014. HIF transcription factors, inflammation, and immunity. *Immunity* 41:518–528. <https://doi.org/10.1016/j.immuni.2014.09.008>.
39. Peyssonnaud C, Datta V, Cramer T, Doedens A, Theodorakis EA, Gallo RL, Hurtado-Ziola N, Nizet V, Johnson RS. 2005. HIF-1alpha expression regulates the bactericidal capacity of phagocytes. *J Clin Invest* 115:1806–1815. <https://doi.org/10.1172/JCI23865>.
40. Blouin CC, Page EL, Soucy GM, Richard DE. 2004. Hypoxic gene activation by lipopolysaccharide in macrophages: implication of hypoxia-inducible factor 1alpha. *Blood* 103:1124–1130. <https://doi.org/10.1182/blood-2003-07-2427>.
41. Phelan JJ, McQuaid K, Kenny C, Gogan KM, Cox DJ, Basdeo SA, O'Leary S, Tazoll SC, OM C, O'Sullivan MP, O'Neill LA, O'Sullivan MJ, Keane J. 2020.

- Desferrioxamine supports metabolic function in primary human macrophages infected with *Mycobacterium tuberculosis*. *Front Immunol* 11: 836. <https://doi.org/10.3389/fimmu.2020.00836>.
42. Cahill C, O'Connell F, Gogan KM, Cox DJ, Basdeo SA, O'Sullivan J, Gordon SV, Keane J, Phelan JJ. 2021. The iron chelator desferrioxamine increases the efficacy of bedaquiline in primary human macrophages infected with BCG. *Int J Mol Sci* 22:2938. <https://doi.org/10.3390/ijms22062938>.
 43. Gokarn K, Pal RB. 2017. Preliminary evaluation of anti-tuberculosis potential of siderophores against drug-resistant *Mycobacterium tuberculosis* by mycobacteria growth indicator tube-drug sensitivity test. *BMC Complement Altern Med* 17:161. <https://doi.org/10.1186/s12906-017-1665-8>.
 44. Lee P, Mohammed N, Marshall L, Abeyasinghe RD, Hider RC, Porter JB, Singh S. 1993. Intravenous infusion pharmacokinetics of desferrioxamine in thalassaemia patients. *Drug Metab Dispos* 21:640–644.
 45. Schofield CJ, Ratcliffe PJ. 2004. Oxygen sensing by HIF hydroxylases. *Nat Rev Mol Cell Biol* 5:343–354. <https://doi.org/10.1038/nrm1366>.
 46. Triantafyllou A, Liakos P, Tsakalof A, Georgatsou E, Simos G, Bonanou S. 2006. Cobalt induces hypoxia-inducible factor-1 α (HIF-1 α) in HeLa cells by an iron-independent, but ROS-, PI-3K- and MAPK-dependent mechanism. *Free Radic Res* 40:847–856. <https://doi.org/10.1080/10715760600730810>.
 47. Jaakkola P, Mole DR, Tian YM, Wilson MI, Gielbert J, Gaskell SJ, von Kriegsheim A, Hebestreit HF, Mukherji M, Schofield CJ, Maxwell PH, Pugh CW, Ratcliffe PJ. 2001. Targeting of HIF- α to the von Hippel-Lindau ubiquitylation complex by O₂-regulated prolyl hydroxylation. *Science* 292:468–472. <https://doi.org/10.1126/science.1059796>.
 48. Catrina SB, Zheng X. 2016. Disturbed hypoxic responses as a pathogenic mechanism of diabetic foot ulcers. *Diabetes Metab Res Rev* 32(Suppl 1): 179–185. <https://doi.org/10.1002/dmrr.2742>.
 49. Hirsila M, Koivunen P, Xu L, Seeley T, Kivirikko KI, Myllyharju J. 2005. Effect of desferrioxamine and metals on the hydroxylases in the oxygen sensing pathway. *FASEB J* 19:1308–1310. <https://doi.org/10.1096/fj.04-3399fje>.
 50. Uygun V, Kurtoglu E. 2013. Iron-chelation therapy with oral chelators in patients with thalassemia major. *Hematology* 18:50–55. <https://doi.org/10.1179/1607845412Y.0000000046>.
 51. Catrina SB, Zheng X. 2021. Hypoxia and hypoxia-inducible factors in diabetes and its complications. *Diabetologia* 64:709–716. <https://doi.org/10.1007/s00125-021-05380-z>.
 52. Bora S, Shankarrao Adole P. 2021. Carbonyl stress in diabetics with acute coronary syndrome. *Clin Chim Acta* 520:78–86. <https://doi.org/10.1016/j.cca.2021.06.002>.
 53. Bento CF, Fernandes R, Ramalho J, Marques C, Shang F, Taylor A, Pereira P. 2010. The chaperone-dependent ubiquitin ligase CHIP targets HIF-1 α for degradation in the presence of methylglyoxal. *PLoS One* 5: e15062. <https://doi.org/10.1371/journal.pone.0015062>.
 54. Ceradini DJ, Yao D, Grogan RH, Callaghan MJ, Edelstein D, Brownlee M, Gurtner GC. 2008. Decreasing intracellular superoxide corrects defective ischemia-induced new vessel formation in diabetic mice. *J Biol Chem* 283: 10930–10938. <https://doi.org/10.1074/jbc.M707451200>.
 55. Thangarajah H, Vial IN, Grogan RH, Yao D, Shi Y, Januszyk M, Galiano RD, Chang EI, Galvez MG, Glotzbach JP, Wong VW, Brownlee M, Gurtner GC. 2010. HIF-1 α dysfunction in diabetes. *Cell Cycle* 9:75–79. <https://doi.org/10.4161/cc.9.1.10371>.
 56. Lemos MP, Rhee KY, McKinney JD. 2011. Expression of the leptin receptor outside of bone marrow-derived cells regulates tuberculosis control and lung macrophage MHC expression. *J Immunol* 187:3776–3784. <https://doi.org/10.4049/jimmunol.1003226>.
 57. Wieland CW, Florquin S, Chan ED, Leemans JC, Weijer S, Verbon A, Fantuzzi G, van der Poll T. 2005. Pulmonary *Mycobacterium tuberculosis* infection in leptin-deficient ob/ob mice. *Int Immunol* 17:1399–1408. <https://doi.org/10.1093/intimm/dxh317>.
 58. Zheng X, Narayanan S, Xu C, Eliasson Angelstig S, Grunler J, Zhao A, Di Toro A, Bernardi L, Mazzone M, Carmeliet P, Del Sole M, Solaini G, Forsberg EA, Zhang A, Brismar K, Schiffer TA, Rajamand Ekberg N, Botusan IR, Palm F, Catrina SB. 2022. Repression of hypoxia-inducible factor-1 contributes to increased mitochondrial reactive oxygen species production in diabetes. *Elife* 11:e70714. <https://doi.org/10.7554/eLife.70714>.
 59. Duscher D, Neofytou E, Wong VW, Maan ZN, Rennert RC, Inayathullah M, Januszyk M, Rodrigues M, Malkovskiy AV, Whitmore AJ, Walmsley GG, Galvez MG, Whittam AJ, Brownlee M, Rajadas J, Gurtner GC. 2015. Transdermal deferoxamine prevents pressure-induced diabetic ulcers. *Proc Natl Acad Sci U S A* 112:94–99. <https://doi.org/10.1073/pnas.1413445112>.
 60. Sugahara M, Tanaka S, Tanaka T, Saito H, Ishimoto Y, Wakashima T, Ueda M, Fukui K, Shimizu A, Inagi R, Yamauchi T, Kadowaki T, Nangaku M. 2020. Prolyl hydroxylase domain inhibitor protects against metabolic disorders and associated kidney disease in obese type 2 diabetic mice. *J Am Soc Nephrol* 31:560–577. <https://doi.org/10.1681/ASN.2019060582>.
 61. Ye Y, Chen Y, Sun J, Zhang H, Li W, Wang W, Zheng X, Catrina SB. 2021. Repressed hypoxia inducible factor-1 in diabetes aggravates pulmonary aspergillus fumigatus infection through modulation of inflammatory responses. *Clin Transl Med* 11:e273. <https://doi.org/10.1002/ctm2.273>.
 62. Joshi N, Caputo GM, Weitekamp MR, Karchmer AW. 1999. Infections in patients with diabetes mellitus. *N Engl J Med* 341:1906–1912. <https://doi.org/10.1056/NEJM199912163412507>.
 63. Haase VH, Glickman JN, Socolovsky M, Jaenisch R. 2001. Vascular tumors in livers with targeted inactivation of the von Hippel-Lindau tumor suppressor. *Proc Natl Acad Sci U S A* 98:1583–1588. <https://doi.org/10.1073/pnas.98.4.1583>.
 64. Clausen BE, Burkhardt C, Reith W, Renkawitz R, Forster I. 1999. Conditional gene targeting in macrophages and granulocytes using LysMcre mice. *Transgenic Res* 8:265–277. <https://doi.org/10.1023/A:1008942828960>.
 65. Xue H, Chen D, Zhong YK, Zhou ZD, Fang SX, Li MY, Guo C. 2016. Deferoxamine ameliorates hepatosteatosis via several mechanisms in ob/ob mice. *Ann N Y Acad Sci* 1375:52–65. <https://doi.org/10.1111/nyas.13174>.
 66. Rothfuchs AG, Gigliotti D, Palmblad K, Andersson U, Wigzell H, Rottenberg ME. 2001. IFN- α beta-dependent, IFN- γ secretion by bone marrow-derived macrophages controls an intracellular bacterial infection. *J Immunol* 167:6453–6461. <https://doi.org/10.4049/jimmunol.167.11.6453>.
 67. Rao Muvva J, Parasa VR, Lerm M, Svensson M, Brighenti S. 2019. Polarization of human monocyte-derived cells with vitamin D promotes control of *Mycobacterium tuberculosis* infection. *Front Immunol* 10:3157. <https://doi.org/10.3389/fimmu.2019.03157>.
 68. Verdon CP, Burton BA, Prior RL. 1995. Sample pretreatment with nitrate reductase and glucose-6-phosphate dehydrogenase quantitatively reduces nitrate while avoiding interference by NADP⁺ when the Griess reaction is used to assay for nitrite. *Anal Biochem* 224:502–508. <https://doi.org/10.1006/abio.1995.1079>.
 69. Carow B, Ye X, Gavier-Widen D, Bhujji S, Oehlmann W, Singh M, Skold M, Ignatowicz L, Yoshimura A, Wigzell H, Rottenberg ME. 2011. Silencing suppressor of cytokine signaling-1 (SOCS1) in macrophages improves *Mycobacterium tuberculosis* control in an interferon- γ (IFN- γ)-dependent manner. *J Biol Chem* 286:26873–26887. <https://doi.org/10.1074/jbc.M111.238287>.